AFCRL-TR-75-0190
PHYSICAL SCIENCES RESEARCH PAPERS, NO. 627

Radiation Effects on Fiber Optics

JAMES A. WALL
JOHN F. BRYANT

2 April 1975

This research was supported by the Air Force In-House Laboratory Independent Research Fund.

SOLID STATE SCIENCES LABORATORY PROJECT ILIR
AIR FORCE CAMBRIDGE RESEARCH LABORATORIES
HANSCOM AFB, MASSACHUSETTS 01731

AIR FORCE SYSTEMS COMMAND, USAF

Unclassified

SECURITY CLASSIFICATION OF THIS PAGE *(When Data Entered)*

REPORT DOCUMENTATION PAGE		READ INSTRUCTIONS BEFORE COMPLETING FORM
1. REPORT NUMBER AFCRL-TR-75-0190	2. GOVT ACCESSION NO.	3. RECIPIENT'S CATALOG NUMBER
4. TITLE *(and Subtitle)* RADIATION EFFECTS ON FIBER OPTICS		5. TYPE OF REPORT & PERIOD COVERED Scientific. Final.
		6. PERFORMING ORG. REPORT NUMBER PSRP No. 627
7. AUTHOR(s) James A. Wall John F. Bryant		8. CONTRACT OR GRANT NUMBER(s)
9. PERFORMING ORGANIZATION NAME AND ADDRESS Air Force Cambridge Research Laboratories (LQR) Hanscom AFB Massachusetts 01731		10. PROGRAM ELEMENT, PROJECT, TASK AREA & WORK UNIT NUMBERS 61101F, ILIR3E Related IHWU: ILIR3E01
11. CONTROLLING OFFICE NAME AND ADDRESS Air Force Cambridge Research Laboratories (LQR) Hanscom AFB Massachusetts 01731		12. REPORT DATE 2 April 1975 13. NUMBER OF PAGES 54
14. MONITORING AGENCY NAME & ADDRESS*(if different from Controlling Office)*		15. SECURITY CLASS. *(of this report)* Unclassified 15a. DECLASSIFICATION/DOWNGRADING SCHEDULE

16. DISTRIBUTION STATEMENT *(of this Report)*
Approved for public release; distribution unlimited.

17. DISTRIBUTION STATEMENT *(of the abstract entered in Block 20, if different from Report)*
1. Fiber Optics -- Radiation Effects

18. SUPPLEMENTARY NOTES
This work was a cooperative effort between AFCRL and NELC. The entire effort was supported by AFCRL Laboratory Director's funds. The NELC portion of the work was performed under Contract MIPR FY71217300017. A portion of the work performed by AFCRL under ARPA Order No. 2490 3D10 is also included in this report.

19. KEY WORDS *(Continue on reverse side if necessary and identify by block number)*
Fiber optics
Radiation effects
Transients

20. ABSTRACT *(Continue on reverse side if necessary and identify by block number)*
The replacement of conventional electrical cables with fiber optics in information transmission systems has the following advantages:

1. No electromagnetic radiation from, or pickup by, cables.
2. Extremely wide bandwidth.
3. Electrical isolation between transmitter and receiver.
4. Smaller size and weight by approximately an order of magnitude.

DD FORM 1 JAN 73 1473 EDITION OF 1 NOV 65 IS OBSOLETE

Unclassified

SECURITY CLASSIFICATION OF THIS PAGE *(When Data Entered)*

These and other advantages are leading to widespread use of fiber optics in military command, communications, and control systems. One problem in the application of fiber optics to military systems is that nuclear (and space) radiation is known to produce color centers in optical materials, causing a reduction of light transmission over a spectrum of wavelengths. Also, energetic radiation can generate light within optical materials. These and other radiation effects could cause permanent or temporary disruption of a fiber optics transmission system.

Samples representative of most of the optical fibers presently available in lengths of 10 m or more were tested for their responses to energetic radiation. Glass fibers doped with three different levels of cesium were also prepared and tested. Permanent and transient x-radiation effects tests were performed using the AFCRL linear accelerator and flash x-ray machine. Neutron effects tests were performed using the fast burst reactor at White Sands, New Mexico.

All of the fibers tested showed decreases in transmission when exposed to radiation. Commercial grade glass fibers were found to be the most radiation sensitive. They became virtually unusuable in lengths greater than 10 m after exposure to only a few hundred rads of x-rays. Considering all of the tests performed, germanium doped fused silica fibers proved to be the least radiation sensitive of the fibers tested. Although their transmission decreased more rapidly with increasing x-ray dose, the plastic fibers showed more rapid recovery from both long-term and transient radiation effects than the germanium doped fused silica fibers. The radiation sensitivities of the cesium doped fibers were intermediate between the commercial grade glass and plastic fibers, with their radiation hardness increasing with increasing cesium doping.

All of the fibers emitted fluorescent light pulses when exposed to intense x-ray pulses. The fluorescent intensity emitted at the ends of the fibers, per unit length of irradiated fiber, was greatest for the commercial grade glass fibers and least for the fused silica fibers. The duration of the fluorescence following an x-ray pulse ranged from less than a microsecond for the plastic and fused silica fibers to several microseconds for the commercial grade and cesium doped glass fibers.

Contents

Contents

Illustrations

Tables

Radiation Effects on Fiber Optics

1. INTRODUCTION

1.1 Background

Interest in replacing conventional electrical cables used in information transmission and control systems with fiber optic light guides has grown considerably in recent years. Transmission systems using fiber optics are similar to those using electrical cables except that the output of the transmitter is used to modulate the intensity of a light source. The source is coupled to one end of an optical fiber which replaces the electrical cable. The other end of the fiber is coupled to a photosensitive device (detector). The detector responds to the light transmitted by the fiber, producing an electrical signal corresponding to the output of the modulated light source. This signal can then be processed as in a system using conventional cables. Some of the advantages of the use of fiber optics in transmission systems are:

(1) No electromagnetic radiation from, or pickup by, cables

(2) Extremely wide bandwidth

(3) Electrical isolation between transmitter and receiver

(4) Smaller size and weight by approximately an order of magnitude

These and other advantages are leading to widespread use of fiber optics in military command, communications, and control systems.

(Received for publication 31 March 1975)

One problem in the application of fiber optics to military systems is that nuclear (and space) radiation is known to produce color centers in optical materials, causing a reduction of light transmission over a spectrum of wavelengths. Also, energetic radiation can generate light within optical materials. These, and other radiation effects could cause permanent or temporary disruption of a fiber optics transmission system. Conventional optical systems contain no more than a few cm of optical material in the light path so radiation effects may be negligible at moderate doses and dose rates. However, systems using fiber optics may have several m, some as much as a km or more, of optical material between the light source and detector. In such systems radiation can produce severe changes in the operation of a system even at relatively low doses and dose rates.

1.2 Program Scope and Objectives

There has been extensive work done in the past on the effects of nuclear radiation on optical materials.[1, 2, 3] However, when this project began there was essentially no information on how radiation affected the performance of optical fibers. The investigation of radiation effects on bulk optical materials that might be used to produce radiation hard optical fibers was considered premature until it was determined whether any effects might occur in the fibers that could not be predicted from prior work. The program was therefore restricted to tests of available optical fibers.

There are many systems, ranging from space vehicles to land based installations, that may utilize fiber optics. Each system must meet radiation tolerance levels below which it must continue to operate for a specified minimum period of time. The lowest tolerance level is for manned systems such as aircraft, land-based communications systems, and naval vessels. These are also the systems in which fiber optics are most likely to be used in the near future. The radiation effects tests were therefore directed primarily toward this tolerance level, which was assumed to be 2000 rads.

Within the above limits, the objectives of this program were:

(1) Evaluate available optical fibers, both commercial and experimental, for their applicability to manned and other systems that may be exposed to energetic radiation.

---

1. Monk, G.S. (1950) The Coloration of Optical Materials by High Energy Radiations, Argonne National Laboratory - 4536.
2. Bishay, Adli (1970) Radiation induced color centers in multicomponent glasses J. Noncrystalline solids 3:54-114.
3. Lell, E., Kreidl, N.J., and Hensler, J.R. (1966) Radiation Effects in Quartz, Silica, and Glasses, Progress in Ceramic Science Vol. 4, Pergamon Press, Oxford.

(2) Determine the requirements for a development program to produce radiation hard optical fibers if needed.

(3) Form a basis to establish radiation effects test procedures for optical fibers.

2. EXPERIMENTAL PROCEDURES

2.1 Technical Approach

The radiation induced transmission losses in optical materials is known to be a nonlinear function of absorbed dose. Because of this nonlinearity the results of radiation effects tests performed on short lengths (1-2 m or less) of optical fibers cannot be reliably extrapolated and applied to systems employing fiber lengths of 30 m or more. It was therefore decided to perform tests on fiber lengths in the range of 10 m. This choice also restricted the tests to those optical fibers being produced in such minimum lengths.

A "live" test procedure was adopted for the permanent damage tests. During these tests the transmission of the fibers was observed continuously during the irradiations. This made possible the observation of any effects, such as the rapid annealing of radiation induced damage, that might occur within time periods of seconds or minutes. Such effects would ordinarily go unnoticed in simple pre- and post-irradiation tests.

The permanent damage tests were performed over only a narrow band of wavelengths corresponding to the emission of a light emitting diode. In order to determine if there were any wavelength regions where radiation induced transmission losses would be minimized, spectral transmission measurements were made on the fibers before and after the irradiations. These spectral measurements could also be used to compare the losses induced in the fibers with published radiation damage data on bulk optical materials to determine if the fiber drawing processes introduced any effects peculiar only to the optical fibers.

Transient radiation effects tests; that is, the responses of the fibers to single high intensity bursts of radiation, were performed with and without light being transmitted through the fibers. This made possible observation of radiation induced fluorescence as well as short term losses of transmission in the fibers. Although attempts were made to determine the spectral distributions of the fluorescence and transmission losses by use of a scanning optical spectrometer, electronic malfunctions that could not be corrected before completion of the project made these measurements impossible.

2.2 Experimental Setup

Figure 1 is a schematic of the experimental arrangement used for the radiation effects tests of the optical fibers. The lengths of fiber were formed into circular coils with outer diameters of approximately 10 cm to insure uniform irradiation over most of the fiber length. One end of the fiber was coupled to a light source and the other end to a photodetector. The source and detector were located in a radiation shielding enclosure that was positioned as far away as practical from the radiation source. The output of the photodetector was connected to an oscilloscope located in the control area. This permitted continuous monitoring of the magnitude of the optical signal transmitted by the fiber during irradiation.

All of the fibers tested were jacketed multifiber bundles (with the exception of a Corning I-279 experimental fiber which was a single fiber). Brass ferules were cemented to the ends of the bundles and the fiber ends ground and polished. Optical coupling to the light source and photodetector was by contact only, no lenses or coupling compounds being used.

For the permanent damage tests the light source used was a pulse modulated light emitting diode (LED) as indicated in Figure 1. The LED was driven by a switching circuit (a Texas Instruments SN7404 integrated circuit) to obtain light pulses of uniform amplitude. The switching circuit was triggered by a pulser, located in the control area, that could be adjusted to set the repetition rate and

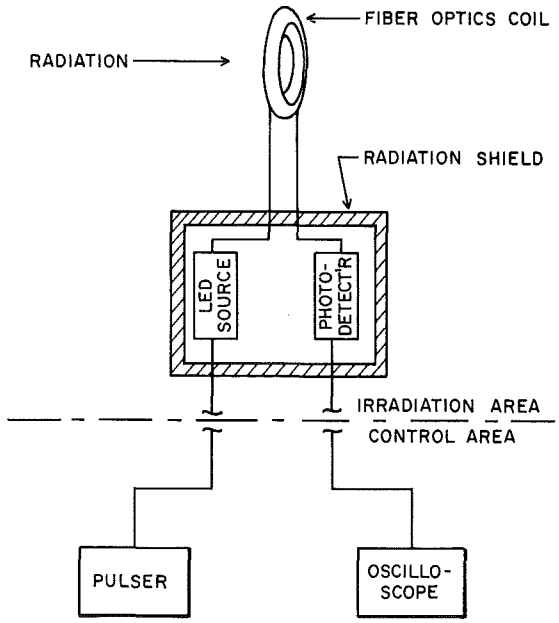

Figure 1. Schematic of Experimental Arrangement

width of the light pulses. An infrared (905 nm) emitting LED (Monsanto ME5) was used during tests of the glass optical fibers. This was replaced by a visible (660 nm) emitting LED for testing plastic fibers which have intense absorption bands in the 900 nm region.

For the transient radiation effects tests the pulse modulated LED was replaced by a high-intensity monochromator (Bausch and Lomb 33-86 series). This provided a constant light source which eliminated the need for pulse synchronization with the single high intensity radiation pulses used in these tests. For glass fibers the monochromator was set for 905 nm and for the plastic fibers 660 nm (both with nominal 10 nm bandwidths) to correspond to the LED emissions used in the permanent damage tests.

The photodetector used was a Texas Instruments TIXL79 avalanche photodiode module. This module has a built-in video amplifier with a bandwidth of 40 MHz. The module responsivity is 2×10^5 volts/watt at 900 nm.

The radiation sources used in the tests were the AFCRL linear accelerator and flash x-ray machine and the fast burst reactor at White Sands Missile Range, New Mexico. The linear accelerator was used for the permanent damage x-ray effects tests. 10 MeV electrons from the accelerator incident on a tungsten target produced 4.5 μsec wide pulses of x-rays. The pulse repetition rate could be varied from manually triggered single pulses to internally generated pulse trains ranging from one to 180 pulses per second. In the position relative to the x-ray target where most of the fibers were irradiated the fibers received about 2 rads (Si) per pulse.

The flash x-ray machine produced bursts of x-rays with a pulse width of 20 nsec. The dose received by the fibers was determined by the distance between the fiber coil and the (internal) machine x-ray target. The doses used in the tests ranged from 20 to 1200 rads per pulse.

The fast burst reactor produced bursts of mixed neutrons and gammas. The bursts were gaussian in shape with a nominal half width of 50 μsec. The neutron fluence received by the fibers was determined by the settings of the reactor control rods, which could be changed from pulse to pulse, and the position of the fiber coil relative to the reactor. For these tests the fibers were located at a distance (100 cm) from the reactor where they would receive neutron fluences ranging from 10^{11} to 10^{12} neutrons/cm^2. The dose received by the fibers due to the gamma radiation from the reactor was typically 2×10^{-10} rad/neutron/cm^2.

The radiation shield indicated in Figure 1 was required to prevent the radiation from reaching the light source and photodetector where it could produce false signals due to transient effects or gradual degradation of the performance of the equipment during prolonged use. For irradiations performed with the linear accelerator the shield wall was a 5 cm thickness of lead; for the flash x-ray machine

it was 10 cm of lead; and for the fast burst reactor it was a composite of about 30 cm of polyethylene, 15 cm of lead, and 0.3 cm of boral.

Thermoluminescent dosimeters (TLD's, CaF imbedded in teflon) were used for dose measurements associated with the linear accelerator and flash x-ray machine. Also, a PIN diode was used for dose-rate monitoring of the linear accelerator and a phosphor-photodiode combination was used to monitor the dose delivered by the flash x-ray machine. Dosimetry at the White Sands fast burst reactor was provided by that facility and employed sulfur pellets for neutron dosimetry and thermoluminescent LiF powder for gamma dosimetry.

Some of the pre- and post-irradiation spectral transmission data on the fibers were taken using "available" spectroscopic equipment pending receipt of a permanent setup. However, most of the spectral data shown in this report were taken using a Bausch and Lomb series 33-86 grating monochromator, silicon photodiode, and PAR lock-in amplifier. An American Time Products type 40 tuning fork chopper, operating at 100 Hz, was located between the tungsten-iodide light source and the entrance slit to the monochromator. One end of the fiber optic bundle was positioned at the exit slit of the monochromator and the other end was coupled to the silicon photodiode. The output of the photodiode was connected to the input of the lock-in amplifier, which was synchronized with the output of the tuning fork drive circuit. Although the entrance and exit slits were set to obtain a 10 nm bandwidth, the actual bandwidth was determined to some degree by the effective apertures of the fibers. However, since only relative spectral transmission data was desired rather than absolute measurements of transmission, this arrangement was adequate for these tests.

2.3 Operational Procedures

2.3.1 PERMANENT X-RAY EFFECTS

2.3.1.1 Irradiation of Fibers

Using the experimental setup described above and shown in Figure 1, the coil of optical fibers was positioned in front of the linear accelerator x-ray target. TLD's were taped to the coil along the vertical and horizontal axes on both the front (facing the target) and back of the coil to obtain a measure of the average dose that would be accumulated by the fiber. The LED was driven with a one μsec wide rectangular pulse with a repetition rate of approximately 200 kHz. Before the irradiation began the signal transmitted by the fiber was observed on the oscilloscope and photographed.

At the beginning of the irradiation the accelerator was manually triggered to obtain single x-ray pulses. During the pulsing the amplitude of the signal transmitted by the fiber was continuously observed on the oscilloscope. When any

significant change occurred in signal amplitude the irradiation was stopped just long enough to photograph the oscilloscope trace. When a fiber did not show a significant change in transmitted signal during the manual pulsing, the accelerator was switched to the internal trigger mode and the pulse rate was slowly increased until the signal began to change at an acceptable rate. As with the manual triggering, the irradiation was stopped to photograph significant changes in signal amplitude. The process of stopping the irradiation to photograph the signal required only a fraction of a second—the time required to switch off the accelerator trigger, trip the camera shutter, and switch on the trigger.

During the irradiations the number of x-ray pulses produced by the accelerator was accumulated on a pulse counter driven by the accelerator trigger circuit. Each time the signal on the oscilloscope was photographed the number of pulses accumulated up to that time was recorded. This information was later used to compute the dose (received by the fiber) that produced the recorded change in signal amplitude. This was done by multiplying the number of pulses generated by the accelerator up to the time the signal was photographed by the dose received by the fiber per x-ray pulse. The dose per pulse was obtained by dividing the total dose accumulated by the fiber during the irradiation, as determined from the TLD's taped to the fiber, by the total number of pulses generated during the irradiation. The PIN diode mentioned in paragraph 2.2 was also used to check the dose per pulse by putting it in place of the fiber and operating the accelerator under the same conditions as during the irradiation.

The irradiations were occasionally interrupted long enough to look for any short-term annealing; that is, recovery of transmission loss, that might occur in a fiber. If annealing was observed the signal trace was photographed at intervals as changes in amplitude occurred. The time between photographs was recorded to obtain data on the annealing process as a function of time.

Also during the irradiations the LED trigger pulse was occasionally turned off to look for fluorescence generated in the fibers by the x-ray pulses. No such fluorescence was observed, however.

The irradiation of a fiber was usually continued until the signal transmitted had dropped in amplitude to between 25 and 50 percent of its original value. The fibers were not usually irradiated to the point where the signal to noise ratio made measurement of the signal amplitude impractical in order to permit measurement of the spectral transmission of the fiber without cutting it to shorter lengths. Cutting the fibers after irradiation in order to make the spectral measurements was not considered desirable because this would mean putting on new end-fittings and repolishing the ends. This, along with possible breakage of some of the fibers in the bundle, could affect the results of the measurements. Only one fiber, the Corning low-loss type A, was irradiated to the point where it had to be cut in order

to make the spectral measurements. When it was desired to determine the induced losses of other fibers as a function of dose at doses greater than required to produce a 50 to 75 percent drop in signal amplitude, the fibers were reirradiated some time after the spectral data was obtained following the first irradiation.

2.3.1.2 Pre- and Post Irradiation Spectral Transmission

Pre- and post-irradiation spectral transmission distributions were measured, with some exceptions as noted below, on the same coils of fibers that were used in the permanent x-ray effects tests. Using the equipment described in paragraph 2.2 monochromator-photodiode "source" spectral distributions were measured by butting together two blank ferules of the type used to terminate the fiber bundles, connecting them between the monochromator and photodiode, and measuring the output of the photodiode as a function of wavelength at 10 nm intervals. The ferules were then replaced with the coiled optical fiber and the process repeated. Dividing the results obtained with the fiber in place by those obtained with the ferules in place gave the relative spectral transmission of the fiber. This procedure was not intended to give an absolute measure of fiber spectral transmission but only to indicate the changes that occurred due to the irradiations.

The exceptions to this procedure were the Corning low-loss type A as mentioned in paragraph 2.3.1.1, the Corning low-loss type B, and the plastic fibers. The type A transmission spectra were measured by comparing the transmission of a 2 m length of fiber with the transmission of a 0.5 m length, the shorter lengths being cut from the coil of fiber before and after irradiation. The post irradiation transmission spectrum of the type B fiber was measured on the full irradiated coil as described above, but the spectrum for the un-irradiated fiber was taken using 2 and 0.5 m lengths taken from the same lot of fiber (this was necessitated by a tight schedule between irradiation sources and a limited supply of the fiber). The plastic fiber transmission spectra were also measured using the shorter lengths of fiber, but the same pieces of fiber were used for both the pre- and post-irradiation measurements. This was done by combining the short lengths of fiber, on which spectral measurements had been made, with the longer coils of fiber during the irradiations. The reason was that these fibers have very intense absorption bands at wavelengths greater than 800 nm. The transmission of the fibers at these wavelengths was too low for measurements to be made on longer lengths of fiber so the shorter lengths were used in order to determine the effects of radiation on the absorption bands.

2.3.2 NEUTRON EFFECTS

The experimental arrangement used at the fast-burst reactor for the neutron effects tests was similar to that used for the permanent x-ray effects tests except as noted in paragraph 2.2. Two oscilloscopes with their inputs connected in

parallel were used to monitor the output of the photodetector. The horizontal sweep trigger of one of the oscilloscopes was delayed approximately 100 μsec with respect to the other (which had no delay) to enable observation of the fiber transmission immediately following a reactor burst. Prior to a burst the oscilloscopes were set for continuous sweep operation and the trace of the signal transmitted by the fiber was photographed. The oscilloscope sweeps were then set to be triggered by a pulse synchronized with the reactor trigger. The oscilloscope camera shutters were manually opened about 1 sec before the reactor was to fire and closed following the burst. This gave photographs of the signal transmitted by the fiber during and immediately following the burst. However, it was found that the electrical noise level during the bursts was very high; so photography of the signal during the bursts (the oscilloscope trace without any time delay) was abandoned although visual observation of that signal was maintained.

Each fiber was exposed to two to four reactor bursts. The sulfur pellets and TLD's used for neutron fluence and gamma dose measurements were left attached to the coil of optical fiber throughout the irradiations so that they measured the accumulated fluence and dose delivered to fiber. The neutron fluence produced by the reactor is directly proportional to the temperature rise of the reactor core during a burst. Photographs, taken by the reactor operating personnel, showing oscilloscope traces of the temperature rise and burst pulse shape were obtained for each reactor burst. Using this information along with the dosimetry data, the neutron fluence at the fiber position was computed for each burst. The gamma dose to the fiber for each burst was similarly obtained since the gamma-neutron ratio is a constant for a fixed position relative to the reactor centerline.

Following each reactor burst the signal transmitted by the fiber was checked at various time intervals to see if any annealing of induced transmission losses occurred. The period over which these observations could be made was usually determined by the minimum required waiting time between reactor bursts. This ranged from 30 min for the lower neutron fluence bursts to 1 hr for the maximum fluence bursts.

2.3.3 TRANSIENT X-RAY EFFECTS

The pulse modulated LED used in the permanent x-ray and neutron effects tests was replaced by a monochromator as mentioned in paragraph 2.2. Although the tungsten-iodide lamp used with the monochromator was powered from a 60 Hz ac line, it provided an essentially constant light source. The coil of fiber to be tested was coupled between the exit slit of the monochromator and the photodetector. The output of the photodetector was connected to the dc input of a wide bandwidth oscilloscope (Tektronix 7904). With the oscilloscope operating on continuous sweep, the displacement of the trace from the zero input signal position

indicated the optical signal level transmitted by the fiber. Although the monochromator entrance and exit slits were set for a nominal 10 nm bandwidth, if a particular fiber did not have enough transmission to provide a signal level adequate for good sensitivity in the tests the entrance slit was widened to provide sufficient signal (the exit slit was not adjustable). Also, if the signal was so large that it could saturate the photodetector, the entrance slit width was reduced to bring the signal within the linear dynamic range of the detector.

As in the permanent x-ray effects tests, TLD's were taped to the fiber coil to measure accumulated dose. The coil was usually positioned relative to the x-ray target so that it would receive approximately 100 rads from a single x-ray pulse. The oscilloscope was set for single sweep operation that could be triggered by a synchronizing pulse from the flash x-ray machine. Before the irradiation, the oscilloscope sweep was triggered by the flash x-ray machine with no x-ray output in order to obtain a photograph of the signal level transmitted by the fiber under actual experimental conditions. The machine was then fired to obtain a photograph of the transient absorption induced by an x-ray pulse. Fibers that did not show a measurable response to the x-ray burst were moved closer to the x-ray target and irradiated with a more intense pulse. The same procedure was followed to measure fluorescence induced in the fibers by x-ray pulses except that an opaque shield was placed between the light source and entrance slit of the monochromator to cut off light input to the fiber.

3. RESULTS

3.1 Data Treatment

All results on radiation induced changes in fiber transmission are reported in units of dB/km. The change in transmission was computed from the relation:

$$\Delta T = \frac{10 \log_{10} S/S_o}{L - \ell} \qquad (1)$$

where

ΔT = change in transmission in dB/km
S_o = amplitude of signal transmitted by fiber before irradiation
S = amplitude of signal after irradiation
L = total length of fiber tested
ℓ = unirradiated length of fiber used as leads between light source and photodetector.

Pre- and post-irradiation spectral measurements are shown as plots of attenuation in dB/km versus wavelength. The attenuation was computed from an equation identical to (1) by redefining the terms as follows:

S_o = signal measured at wavelength λ with shorter length of fiber in spectrometer

S = signal measured at wavelength λ with longer length of fiber in spectrometer

ℓ = shortest length of fiber in km

L = longest length of fiber in km

For spectral measurements on the full fiber coils used in the tests S_o becomes the source detector function of the spectrometer and $\ell = 0$.

As previously stated in paragraph 2.2, the spectral transmission measurements were intended to yield only relative attenuation data. In order to show the relative change between the pre- and post-irradiation spectra in relation to the change in transmission observed during irradiation, the post-irradiation spectra were adjusted relative to the pre-irradiation spectra. This was done by taking the difference (in dB/km) between the two spectra at the light-source wavelength used during the irradiation. This was compared with the change in transmission observed at the end of the irradiation. The entire post-irradiation spectrum was then adjusted by adding or subtracting the appropriate number of dB/km to obtain agreement between the spectral results and the irradiation results at the appropriate wavelength. This correction was usually less than 10 percent of the attenuation measured in the post-irradiation spectrum at the wavelength in question.

The optical fibers tested can be classified into four types as follows:

(1) Commercial Grade Glass Fibers. These are general purpose fibers available as stock items from manufacturers. They are drawn from "standard" optical glasses such as lead silicate and have intrinsic attenuations of the order of 1000 dB/km.

(2) Low-loss Fused Silica Fibers. These are drawn from pure fused silica with a dopant added to the core to increase its refractive index. Intrinsic attenuation is less than 100 dB/km.

(3) Plastic fibers. These are very inexpensive fibers with cores of either polymethylmethacrylate or polystyrene and a clad of lower refractive index polymer. They have very high attenuation at wavelengths greater than 800 nm. Their attenuation in the visible is about 1200 dB/km.

(4) Cerium-doped fibers. These are glass fibers made by adding a small amount of cerium oxide to the glass melt before they are drawn to increase their resistance to radiation induced transmission losses. (Cerium doped glass has been used for several years to produce hot-cell windows and optical components

for use in high-level radiation areas). The cerium doped fibers tested were specially made for this project and had initial attenuations of approximately 1200 dB/km.

The radiation effects observed were distinctly different for each type of fiber. The results of each radiation test are therefore reported according to fiber type.

3.2 Permanent X-Ray Effects

3.2.1 COMMERCIAL GRADE GLASS FIBERS

Three commercial grade glass fibers were tested. These were the Bendix K2K, * Rank Hi-Tran, and Schott LK fibers. The results of the radiation tests are shown in Figures 2, 3, and 4 where the observed change in fiber transmission is plotted against the dose received by the fiber. The fibers were initially irradiated until their transmissions dropped to about 50 percent of the pre-irradiation levels. Forty days later the fibers were recoupled to the same LED and photodetector and irradiated again until the transmitted signal was too small for accurate measurements to be made. The time interval between irradiations is indicated on the plots. As can be seen in the figures, the Bendix K2K fiber had regained some of its transmission loss during the time interval between irradiations. The Rank Hi-Tran showed no significant change in transmission during the time interval while the Schott LK data indicate a decrease in transmission. This latter effect, however, could be and probably is due to a slight difference in the coupling of the fiber to the LED and photodetector between the two irradiations.

Least-square fits were made to these data and are shown as the straight lines through the data points on the plots. The change in transmission is a closely linear function of dose over the range of exposures used in these tests. (Since change in transmission is expressed here in dB/km, this means that the amplitude of the transmitted signal changes exponentially with dose). The slopes of these lines, indicated on the plots, can be used as a relative measure of the radiation hardness of the fibers. The slopes of the lines through the Bendix and Rank fiber data are very nearly the same and are significantly greater than the slope of the line through the Schott fiber data. Although the Schott fiber is less sensitive to radiation than the other two, it is clear from the data that none of these fibers would remain useable (except in much shorter lengths than tested) if exposed to the 2000 rad dose tolerance limit assumed for manned systems.

Figures 5, 6, and 7 show the pre- and post-irradiation spectral transmissions of the Bendix, Rank, and Schott fibers respectively. The pre-irradiation spectra

---

*The Bendix optical fiber production facilities had been taken over by the Galileo Electro Optics, Inc., when these tests were performed. However, the Bendix name is retained in this report because the fiber tested was so labeled.

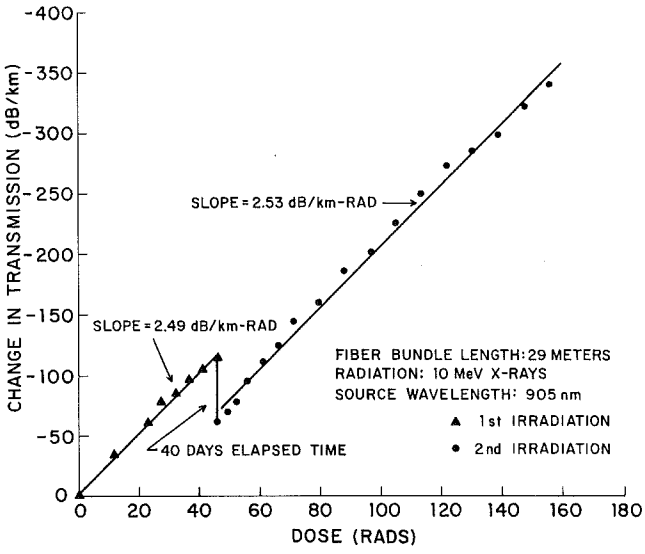

Figure 2. Change in Transmission Versus Dose, Bendix K2K

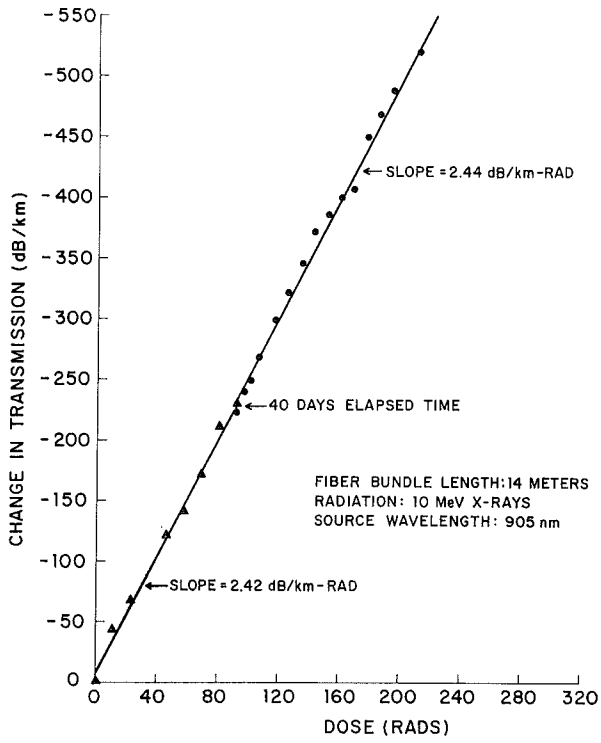

Figure 3. Change in Transmission Versus Dose, Rank Hi-Tran

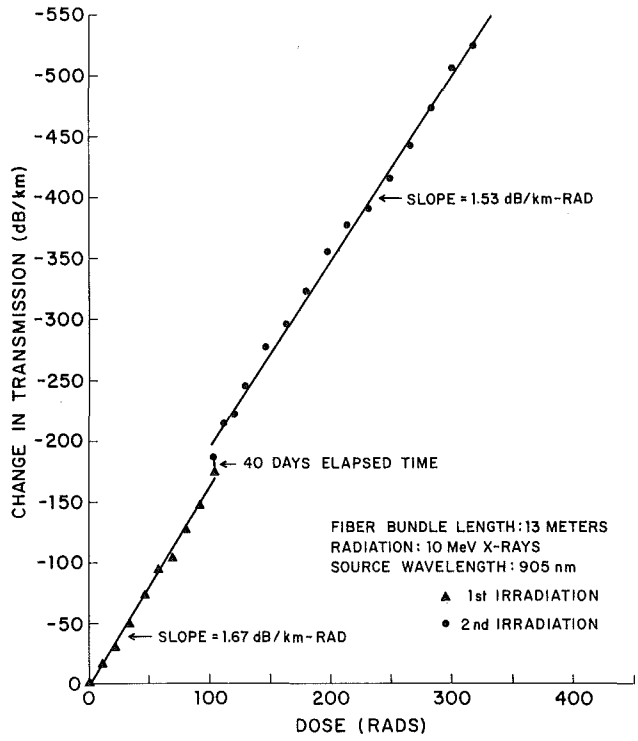

Figure 4. Change in Transmission Versus Dose, Schott LK

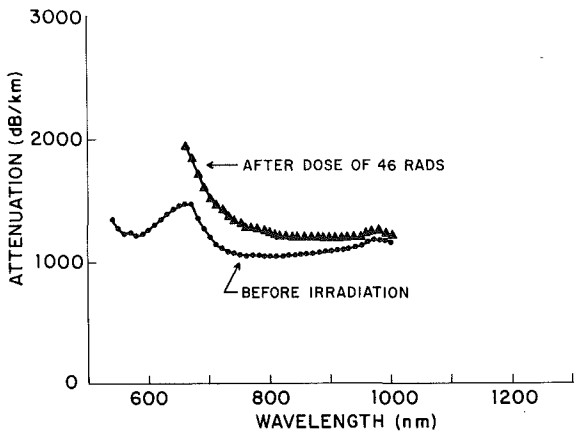

Figure 5. Attenuation Versus Wavelength, Bendix K2K

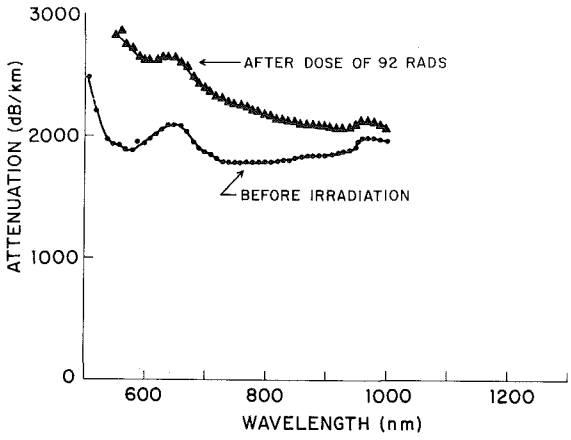

Figure 6. Attenuation Versus Wavelength, Rank Hi-Tran

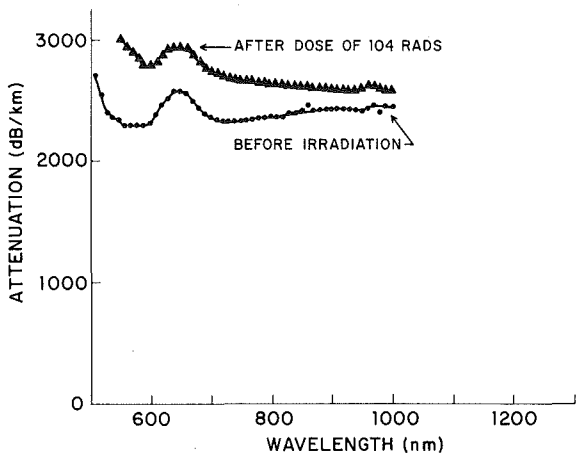

Figure 7. Attenuation Versus Wavelength, Schott LK

are all very similar, with absorption bands near 650 and 970 nm. This similarity suggests that the core glass is of one type for all three fibers. Differences in radiation response between the fibers such as the greater radiation hardness of the Schott and the annealing characteristic of the Bendix are probably due to minor differences in the elemental compositions of the glasses. The post-irradiation spectra show a greater increase in attenuation at the shorter wavelengths than at longer wavelengths. This is typical of the radiation induced attenuation in most glasses and suggests that the results of radiation effects tests of bulk glasses can be applied to optical fibers drawn from them. This of course assumes that no impurities are introduced during the drawing process.

3.2.2 LOW-LOSS FUSED SILICA FIBERS

Three types of low-loss fused silica fibers, all manufactured by Corning Glass Works, were tested. Two of these were designated by the manufacturer as low-loss type A and low-loss type B and were supplied as jacketed multiple-fiber bundles. The third was an experimental prototype of the low-loss type B. This was a single fiber labeled as I-279. Although the compositions of these fibers are not known in detail, it is known that the core of the type A fiber is doped with titanium while the cores of the type B and I-279 are doped with germanium.

Figure 8 shows the results of the irradiation of the low-loss Type A. No data was taken below the 220 rad dose level, but for the higher doses the change in transmission appears to be a linear function of dose. (The irradiation was actually continued to a dose of 1000 rads although this is not shown in Figure 8). A least-squares fit to the data above 220 rads gave a slope of 0.74 dB/km-rad as indicated

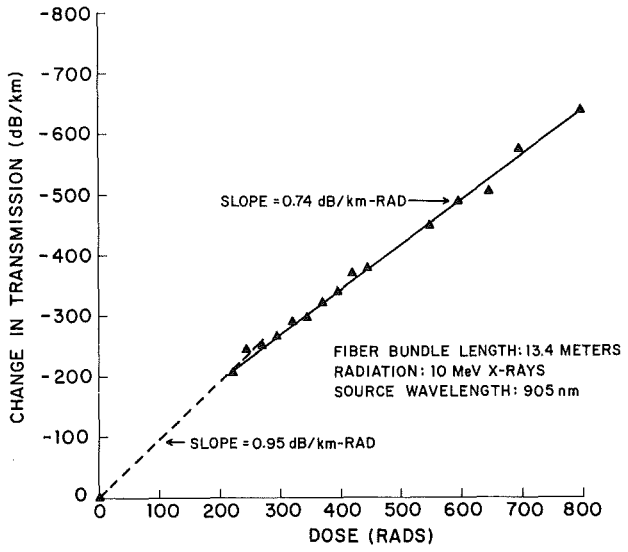

Figure 8. Change in Transmission Versus Dose, Corning Low-Loss "A"

on the plot. This fiber is therefore less than half as sensitive to radiation as the commercial glass fibers but still is not sufficiently radiation resistant to be used in manned systems.

The test results for the low-loss type B are shown in Figure 9. The response of this fiber to radiation is clearly different than either the commercial glass fibers or the low-loss type A. It is much more resistant to radiation damage than the others. The initial slope of the curve drawn through the data points is approximately 3×10^{-3} dB/km-rad, about three orders of magnitude less than the other fibers. Some annealing of the radiation induced transmission loss was also found and is indicated in Figure 9 by the data points at 20 kilorad and 160 kilorad. After the fiber had received a dose of 20 kilorad, the irradiation was stopped for 15 min and the induced transmission loss was observed to drop from 58 to 50 dB/km. The irradiation was then continued until the fiber had received a total dose of 160 kilorad. At this point the signal transmitted by the fiber had dropped in amplitude to about 50 percent of its original magnitude, corresponding to a change in transmission of 228 dB/km. Seventeen hours later the signal amplitude had recovered to 87 percent of its original value. This represents a transmission loss of only 50 dB/km, a 178 dB/km decrease in loss since the irradiation was stopped. The LED was turned off during the 17 hr waiting period. The observed annealing was therefore intrinsic to the fiber and not induced or enhanced by the light source.

The nonlinearity of the change in transmission as a function of dose of the low-loss type B also distinguishes it from the commercial glass and type A fibers. (However, those fibers could not be irradiated to the dose levels received by the type B because of their rapid loss in transmission. If they had been, they

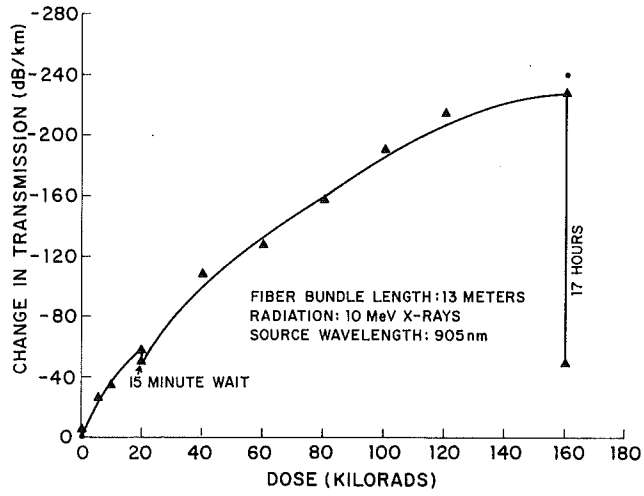

Figure 9. Change in Transmission Versus Dose, Corning Low-Loss "B"

might also have shown non-linear responses.) As will be seen below from the results obtained in the tests of plastic fibers, an apparent nonlinear response could result from a combination of the rate at which the transmission loss annealed and the rate at which the dose was delivered to the fiber. During the irradiation of the type B fiber the linear accelerator was operated at a pulse repetition rate of about 20 pulses per second with a dose of 2 rads per pulse at the fiber position. It is possible that during the 50 ms period between pulses some of the loss induced by the individual x-ray pulses annealed out. For this to cause the observed nonlinearity the annealing rate immediately following an x-ray pulse would have to be much greater than the rate observed when the irradiation was stopped.

Figure 10 shows the results obtained for the I-279 fiber. This fiber was tested especially for the Defense Advanced Research Projects Agency and the results of those tests are reported elsewhere.[4] The data is shown here for comparison with the type B low-loss fiber. The greater scatter in the data points obtained with this fiber as compared with the others is probably due to the sensitivity of the coupling of the single fiber to its position relative to the light source and photodetector. Minor vibrations and air currents in the irradiation area that would not affect the fiber bundles could have a significant effect on the stability of the coupling of the single fiber. Within such experimental variables, however, the radiation response of the I-279 is similar to that of the low loss type B.

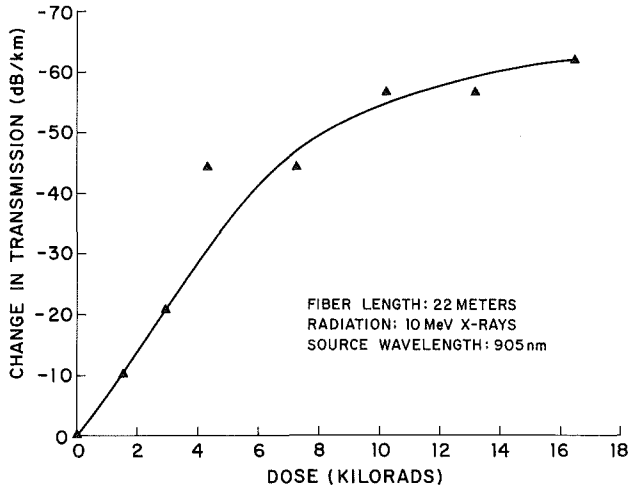

Figure 10. Change in Transmission Versus Dose, Corning I-279

4. Wall, J.A. (1975) Transient Radiation Effects Tests of a Corning Radiation Resistant Fiber, AFCRL-TR-75-0012.

No annealing of the induced transmission loss was observed in the I-279, but only short periods of time (10-15 min) were allowed for observation of this effect. It was not possible to have the fiber in position for several hours as in the case of the type B to check for long-term annealing.

Figures 11 and 12 show the pre- and post-irradiation transmission spectra for the low-loss types A and B respectively. As in the case of the commercial glass fibers, both post-irradiation spectra show large increases in absorption at the shorter wavelengths. The absorption induced in the type B, however, decreases much more rapidly toward the longer wavelengths than does the absorption induced in the type A. Although the type B is more radiation resistant than the type A even at the shorter wavelengths, the difference between the two is significantly enhanced in the near infrared because of this more rapid decrease in the induced absorption.

3.2.3 PLASTIC FIBERS

Two types of plastic optical fibers were tested: Dupont Crofon® 1110 and International Fiber Optics 1032. The Dupont fiber has a polymethylmethacrylate core and the International has a polystyrene core. Most, if not all, of the plastic optical fibers available are made with one of these core materials. Tests of other plastic fibers were therefore not considered necessary.

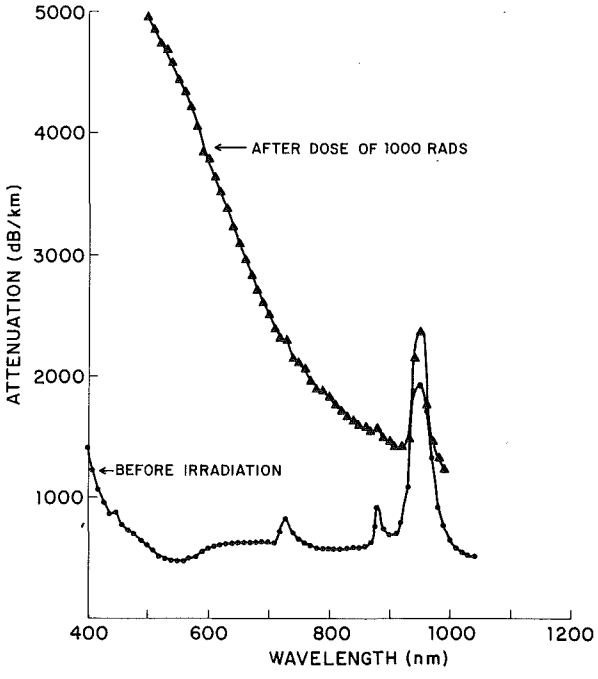

Figure 11. Attenuation Versus Wavelength, Corning Low Loss "A"

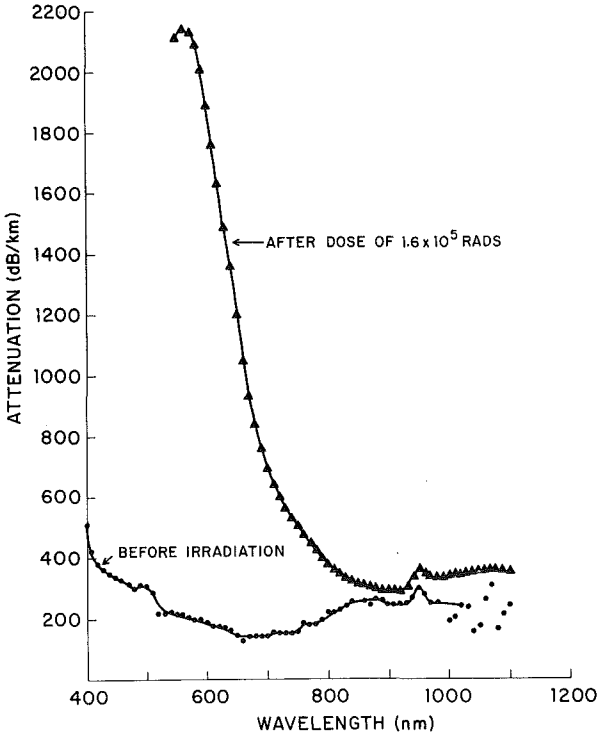

Figure 12. Attenuation Versus Wavelength, Corning Low Loss "B"

Figure 13. Change in Transmission Versus Dose, Dupont Crofon R 1110

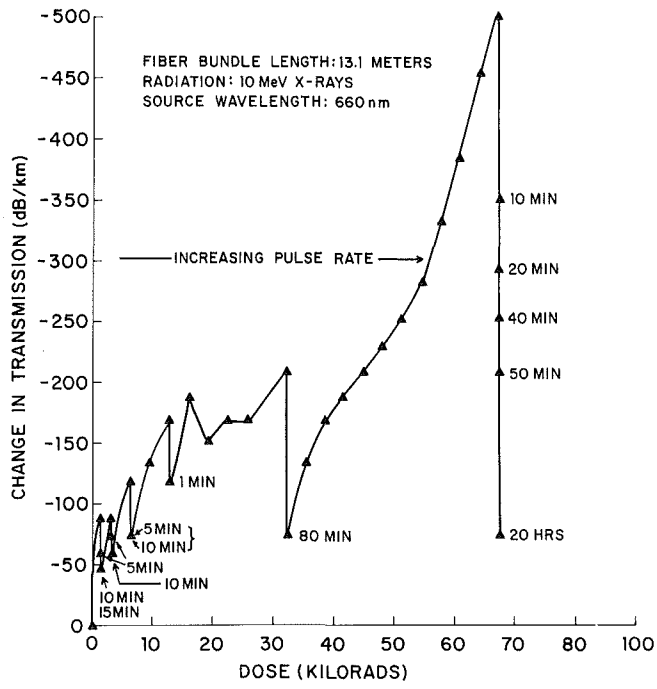

The test results for the Dupont Crofon® are shown in Figure 13. The time intervals shown on the plot at different doses are points at which the irradiation was stopped to observe annealing of the induced transmission loss. The indicated time intervals are the accumulated times following cessation of the irradiation. For example, at 67 kilorad the first point below the maximum was taken 10 min after the irradiation was stopped, the second point 20 min after the end of irradiation, etc. The data show that annealing of the induced transmission loss proceeded fairly rapidly, sufficiently so that the results obtained were dependent on the rate at which the linear accelerator was pulsed. Unfortunately, during the irradiation this effect was not anticipated and an accurate record of the pulse repetition rate was not kept. When the induced transmission loss appeared to be changing too slowly, the pulse rate was increased until the signal amplitude began to change at an acceptable rate. The maximum pulse repetition rate used, however, was 60 pulses per sec and this applies in the region between 55 and 67 kilorad. The dose per pulse was 3.2 rads.

The test results for the International Fiber Optics fiber are shown in Figure 14. In this case the relationship between the annealing rate and the accelerator pulse rate was anticipated. As Figure 14 shows, the irradiation was continued at a fixed pulse rate until the induced transmission loss stopped increasing with accumulated dose. The pulse rate was then increased and the

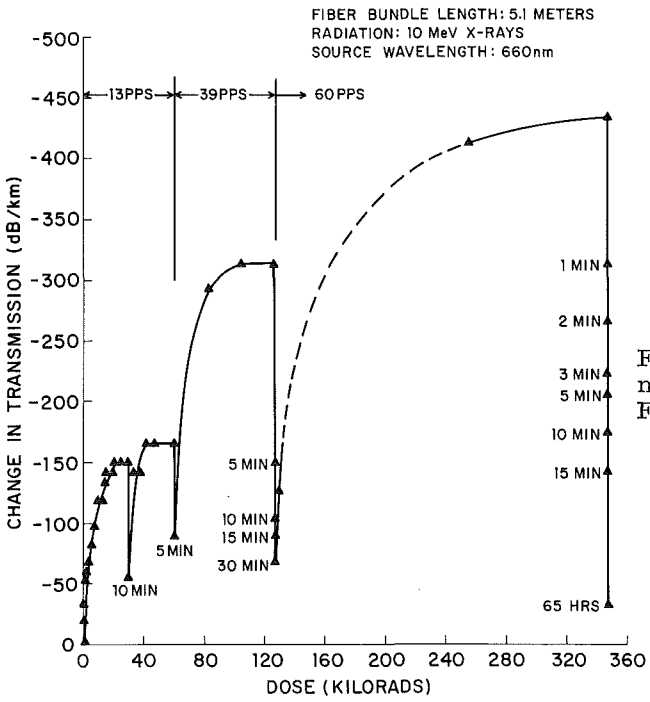

Figure 14. Change in Transmission Versus Dose, International Fiber Optics 1032

procedure repeated. Periodic stops of the irradiation to observe annealing are indicated on the plot. For this irradiation the dose per pulse was 2.2 rads.

An interesting feature of the data shown in Figures 13 and 14 is that, following each annealing period, the initial slopes, that is, rates of change in transmission with dose of the curves are approximately the same regardless of the pulse repetition rate. For both fibers the slope is about 0.02 dB/km-rad. This suggests that the initially induced transmission loss is proportional to accumulated dose. However, as is most obvious from the International Fiber Optics fiber data, the equilibrium transmission loss attained is a function of pulse rate. The rate of annealing of the induced transmission loss must therefore be a function of the induced loss. For example, referring to Figure 14, at a pulse rate of 13 pps equilibrium was reached at a loss of 165 dB/km. For equilibrium to occur the loss induced by each pulse must have annealed out shortly before the next pulse arrived, in this case in 0.077 sec. At 39 pps, the loss induced by a single pulse had to anneal out in 0.026 sec at the 365 dB/km level. Because of the strong dependence of annealing rate on induced loss, the results of these and other radiation effects tests of plastic fibers must be examined with respect to the environment in which the fiber is to be used. For a potential nuclear weapons environment, transient radiation effects tests should yield more applicable data than the permanent effects tests.

The long-term annealing data shown in Figures 13 and 14 can be used to estimate the extent of recovery of the induced transmission loss following the end of an irradiation. The ratios of the losses observed at the indicated times after the irradiation was stopped were calculated with respect to the induced loss observed immediately at the end of the irradiation. A log-log plot of the ratios versus time yielded a straight line, as shown in Figure 15, for the International Fiber Optics data. The ratios (relative transmission losses) shown on the plot combine the

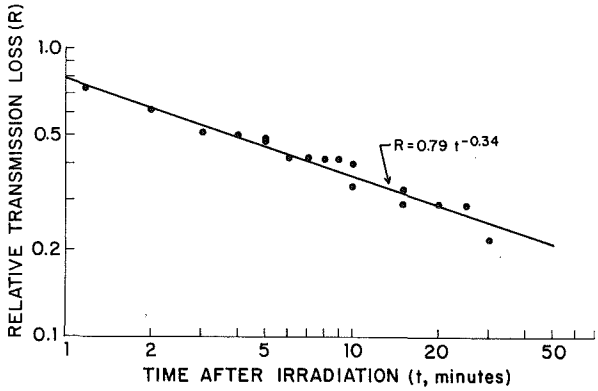

Figure 15. Relative Induced Transmission Loss Versus Time After Irradiation, International Fiber Optics 1032

annealing data taken at 127 kilorads and 347 kilorads. A least-squares fit to the data gave the relationship:

$$R = 0.79\ t^{-0.34} \tag{2}$$

where R is the ratio of the induced loss at time t (minutes) after the irradiation was stopped to the loss observed before significant annealing occurred. Similarly, the relationship

$$R = 1.4\ t^{-0.3} \tag{3}$$

was obtained from the Crofon® data

Equations 2 and 3 obviously cannot be applied to annealing times shorter than those for which R = 1. For Eq. (2), t cannot be less than 0.5 min and for Eq. (3) t cannot be less than 3 min. Also, (2) and (3) do not take into account damage that does not anneal out and both give results that are low by approximately a factor of two for the 20 hr and 65 hr annealing times.

Figures 16 and 17 show the pre- and post-irradiation transmission spectra for the Crofon® and International Fiber Optics fibers respectively. Within the accuracy of the measurements, the Crofon® spectrum was essentially unchanged by the irradiation except for a slight decrease in the intensity of the absorption bands at wavelengths greater than 850 nm. A radiation induced increase in attenuation at wavelengths below 650 nm is the only significant change observed in the International Fiber Optics transmission spectrum.

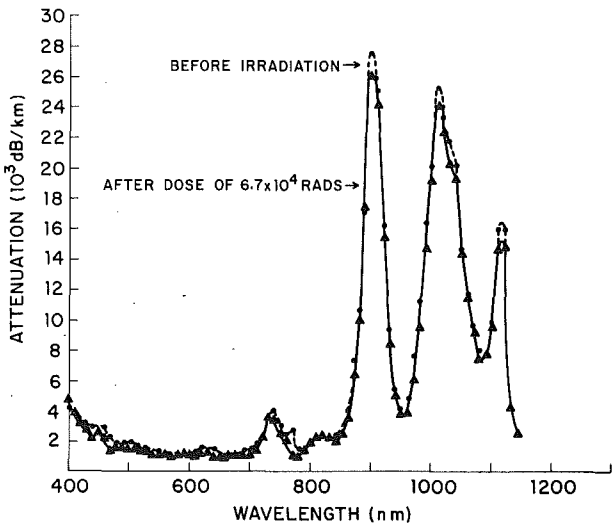

Figure 16. Attenuation Versus Wavelength, Dupont Crofon® 1110

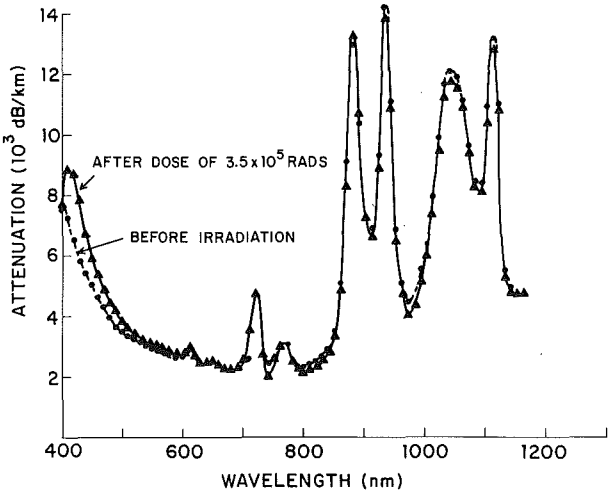

Figure 17. Attenuation Versus Wavelength, International Fiber Optics 1032

3.2.4 CERIUM DOPED FIBERS

Cerium doped optical fibers were specially prepared for this project by Galileo Electro-Optics Corp. The base glass from which the fibers were drawn was zinc crown. Three different glass melts doped with 0.1, 0.2, and 0.3 percent cerium were prepared and fibers drawn from them. The fibers were supplied as 15 m long jacketed bundles each containing approximately 100 fibers. The intrinsic attenuations of the fibers as determined by the manufacturer were 1250, 1200, and 1500 dB/km for the 0.1, 0.2, and 0.3 percent derium doping respectively.

The results of the tests of the cerium doped fibers are shown in Figure 18. All three fibers are much more resistant to radiation induced transmission losses than the commercial glass fibers and there is a significant increase in this resistance with increasing cerium doping. Comparison of the data for the 0.1 percent and 0.2 percent cerium doped fibers shows that the extent to which the induced losses annealed out also increased with increased cerium doping. Both fibers were irradiated until the induced loss was about 400 dB/km. Sixty-eight hours after the irradiation the 0.2 percent doped fiber had regained 225 dB/km of the induced loss while the 0.1 percent doped fiber had regained only 100 dB/km 66 hr after the irradiation. It is not clear from the data whether or not increasing the cerium doping from 0.2 to 0.3 percent improved the degree of annealing because the 0.3 percent doped fiber was not irradiated to as high an induced loss as the other two fibers. However, the 0.3 percent fiber regained 200 dB/km of the induced loss 67 hours after the irradiation, which is about the same as for the 0.2 percent doped fiber, suggesting that the additional cerium doping did not significantly affect the extent of annealing.

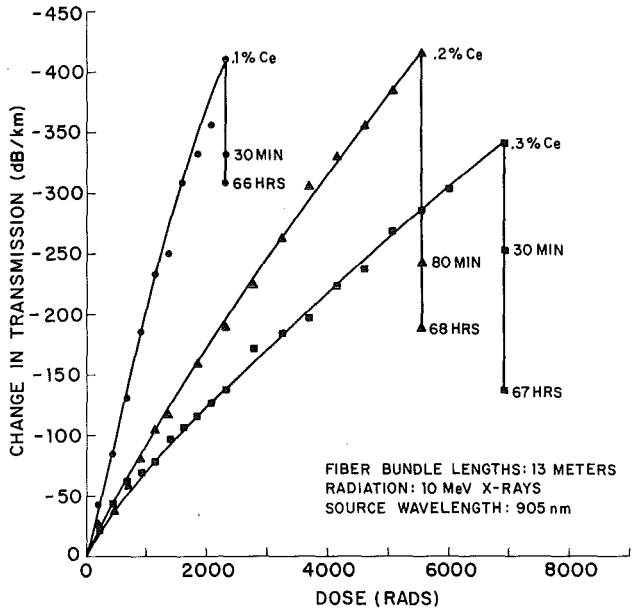

Figure 18. Change in Transmission Versus Dose, Cerium Doped Glass Fibers

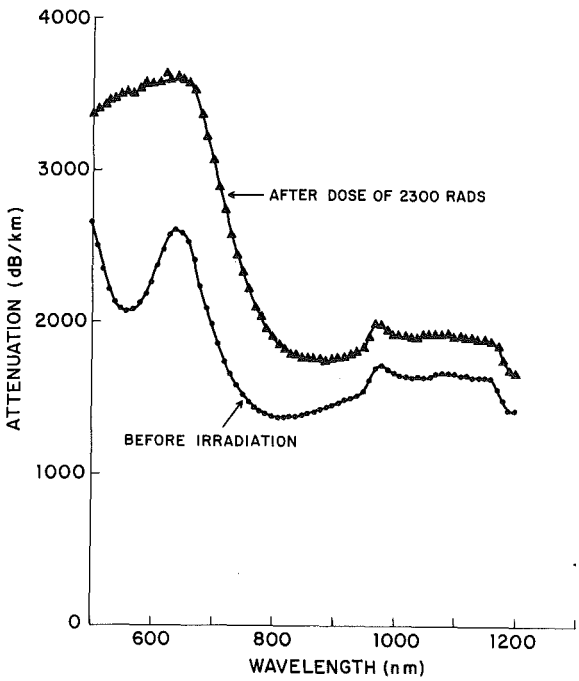

Figure 19. Attenuation Versus Wavelength, 0.1 percent Cerium Doped Glass Fiber

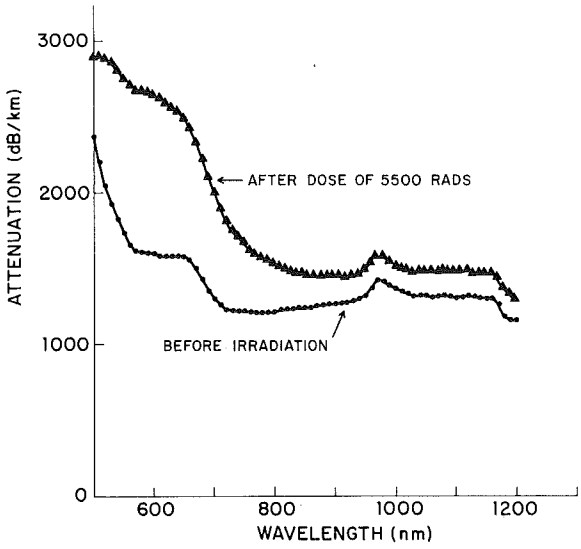

Figure 20. Attenuation Versus Wavelength, 0.2 percent Cerium Doped Glass Fiber

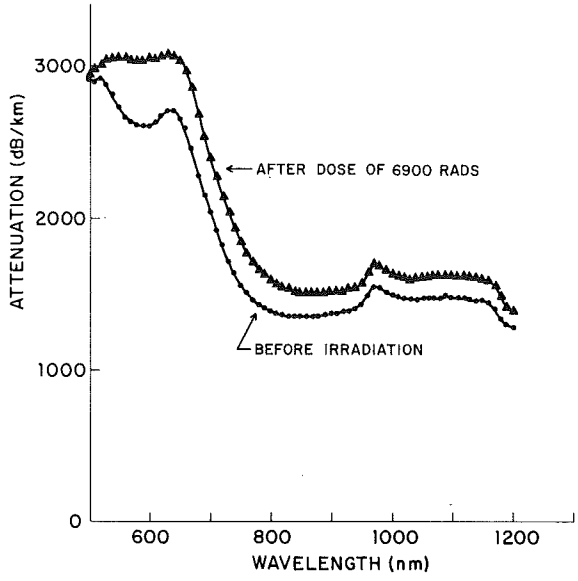

Figure 21. Attenuation Versus Wavelength, 0.3 percent Cerium Doped Glass Fiber

The slopes of the curves drawn through the data points in Figure 18 decrease with increasing dose. As in the case of the Corning low-loss type B (paragraph 3.2), it cannot be certain whether the indicated nonlinear relationship between induced change in transmission and dose is characteristic of the fibers or is due to rapid partial annealing of the induced losses between x-ray pulses.

Figures 19, 20, and 21 show the pre- and post-irradiation spectra for the cerium doped fibers. The pre-irradiation spectra clearly show the absorption bands resulting from the cerium doping at wavelengths below 700 nm. The post-irradiation spectra show the broadening of these bands caused by the trapping of electrons generated during irradiation. At wavelengths greater than 900 nm the separation between the pre- and post-irradiation spectra for each fiber remains very nearly constant. This means that the radiation hardness of this type of fiber is essentially independent of wavelength between 900 and (at least) 1200 nm.

3.2.5 RELATIVE SENSITIVITIES OF FIBERS TO X-RAYS

The initial slopes of the plots of radiation induced change in transmission versus dose may be used to estimate the relative sensitivies of the fibers tested to damage by x-rays. The slopes correspond to the rate of increase in loss of transmission with increasing accumulated dose. The initial slopes were chosen for this comparison because they start at "zero-dose", a common reference point for all irradiations, and avoid the ambiguities involved in the nonlinear responses observed with some of the fibers. Table 1 shows the slopes (initial rate of induced loss) obtained from the fiber test results.

Table 1. Comparison of Sensitivities of Fibers to X-Radiation

Fiber Type	Fiber Designation	Initial Rate of Induced Loss (db/km-rad)
Commercial Glass	Bendix K2K	2.49
	Rank Hi-Tran	2.42
	Schott LK	1.67
Low-Loss Fused Silica	Corning Low-Loss "A"	0.95
	Corning Low-Loss "B"	3.4×10^{-3}
	Corning I279	5.6×10^{-3}
Plastic Fibers	Dupont Crofon®	0.055
	International Fiber Optics 1032	0.035
Cerium Doped Fibers	0.1 percent Ce	0.2
	0.2 percent Ce	0.084
	0.3 percent Ce	0.079

Comparison of the initial rates of induced loss is obviously not a perfect measure of the relative radiation sensitivities of optical fibers. For example, Figure 18 shows the 0.3 percent cerium doped fiber to be much less sensitive to radiation compared to the 0.2 percent cerium doped fiber than the rates of induced loss shown in Table 1 imply. However, Table 1 clearly shows that the germanium doped fused silica fibers (Corning Low-Loss "B" and I-279) are the least sensitive to x-radiation of the fibers tested. These are followed by the plastic fibers, the cerium doped fibers, the titanium doped fused silica fiber (Corning Low-Loss "A"), and the commercial glass fibers in order of increasing radiation sensitivity. If fast annealing of induced loss is considered an important factor in determining the radiation hardness of a fiber, the plastic fibers would be chosen as the least sensitive to radiation. Such information is not shown in Table 1 and must be obtained by reference to the original data.

3.3 Neutron Effects

3.3.1 COMMERCIAL GRADE GLASS FIBERS

Two commercial grade glass fibers were tested for their responses to neutrons. These were Bendix K2K and Corning 5011 fibers. The results of the tests are shown in Figures 22 and 23 respectively. For these and other

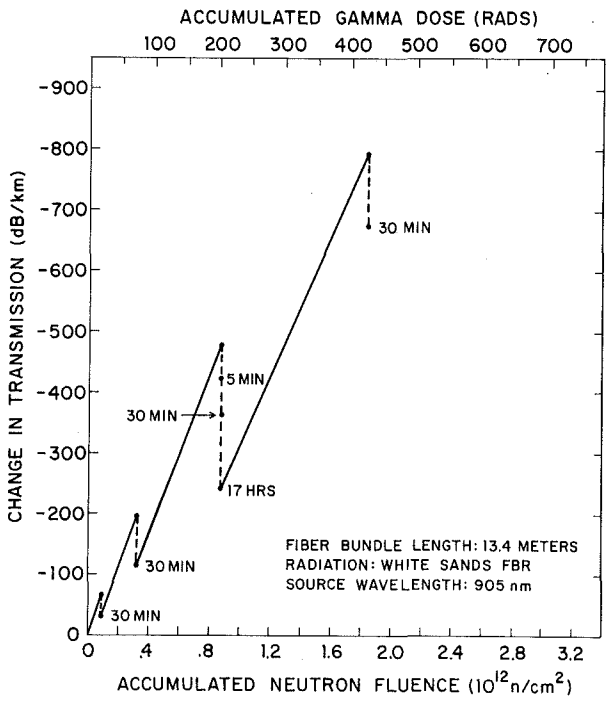

Figure 22. Change in Transmission Versus Neutron Fluence, Bendix K2K

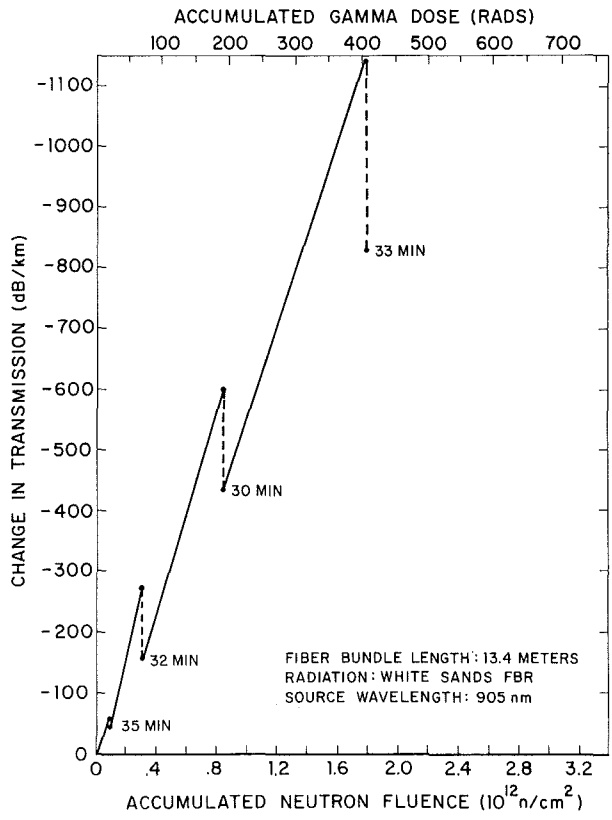

Figure 23. Change in Transmission Versus Neutron Fluence, Corning 5011

representations of the neutron effects data, the data point at the upper end of each line segment represents the change in signal transmission measured immediately following a reactor burst. The data points below this represent the change in transmission measured at the indicated times following the burst. The lower abscissa gives the sum of the neutron fluences at the fiber for all bursts up to the indicated data points and the upper abscissa is the corresponding sum of the gamma doses in rad (Si) for the bursts.

For the Bendix K2K data (Figure 22) the average slope, relative to accumulated gamma dose, of the lines drawn between data points is 2.5 dB/km-rad. This is almost identical to the initial rate of induced loss (2.49 dB/km-rad) found in the x-ray effects tests (see Table 1, paragraph 3.2.5). It may therefore be concluded that the induced losses observed were produced primarily by the gamma radiation associated with the reactor bursts and that the neutrons caused relatively little change in transmission. The neutrons apparently had a significant affect on the annealing of induced loss, however. No short term annealing was observed during the permanent x-ray effects tests of this fiber, although 40 days after the first irradiation the induced change in transmission dropped from 114 to 62 dB/km (see Figure 2, paragraph 3.2.1). The data in Figure 22 show much more rapid

annealing. For example, after an accumulated neutron fluence of 3.3×10^{11} neutrons/cm^2 and gamma dose of 74 rads, the induced change in transmission dropped from 197 to 115 dB/km in 30 min.

The data for the Corning 5011 shown in Figure 23 is similar in form to the Bendix K2K data. Since no permanent x-ray effects tests were performed on the 5011, a comparison of the effectiveness of the gamma radiation relative to the neutrons in producing damage in the fiber is not possible. Neither can any conclusions be drawn regarding possible neutron-induced increases in annealing rate. However, it was found in the transient x-ray effects tests that the rate of induced loss for the 5011 was about 40 percent higher than for the K2K. The average slope, relative to gamma dose, of the lines between data points in Figure 23 is 3.7 dB/km-rad. Increasing the average slope for the K2K data by 40 percent gives 3.5 dB/km-rad. The closeness of these two values makes it reasonable to conclude that the relative gamma-neutron response of the Corning 5011 is similar to that of the Bendix K2K.

3.3.2 LOW-LOSS FUSED SILICA FIBERS

The Corning low-loss type B and I-279 germanium doped fused silica fibers were tested. The I-279 single fiber was exposed to three successive reactor bursts, each producing a neutron fluence of 1.0×10^{12} n/cm^2 and a gamma dose of 217 rad at the fiber position. No change in the amplitude of the signal transmitted by the fiber was observed immediately following any of the bursts. The amplitude of the signal from the photodetector was low, however, and it is possible that small changes in amplitude occurred that could not be measured.

The results of the low-loss type B irradiation are shown in Figure 24. Malfunctions of the oscilloscope camera prevented measurement of the signal amplitude immediately following the second and fourth reactor bursts. The delays of 3 min and 1 min that occurred before the signal was photographed are indicated in Figure 24. The data at 1.2×10^{11} neutrons/cm^2, taken after the first burst, show that significant annealing probably occurred during these delay times. Also, 45 min elapsed between the second and third bursts and no photograph of the signal was obtained to determine the amount of annealing that could have occurred during this period. Dashed lines are shown connecting these data points to indicate that they should not be used to determine rates of induced loss.

In spite of these problems, the data shown in Figure 24 can be used to draw some conclusion about the effects of neutrons on the low-loss type B fiber. The slope, relative to gamma dose, of the line drawn from the origin to the first data point at 1.2×10^{11} n/cm^2 and 31 rads is 0.98 dB/km-rad. This is considerably greater than the initial rate of induced loss of 3.4×10^{-3} dB/km-rad determined in the permanent x-ray effects tests of this fiber. It may be concluded from this

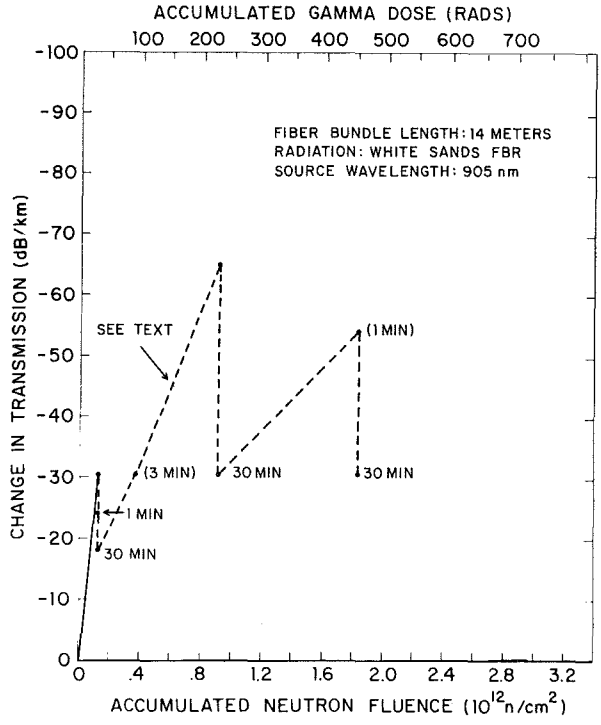

Figure 24. Change in Transmission Versus Neutron Fluence, Corning Low-Loss "B"

that, unlike the commercial glass fibers, the neutrons rather than gamma radiation are the primary cause of induced change in transmission for this fiber.

The data point at 9×10^{11} n/cm^2 and an induced change in transmission of 65 dB/km was taken immediately following a reactor burst. Thirty minutes later the transmission had improved by over 34 dB/km. Judging from the data at 1.2×10^{11} n/cm^2, most of this annealing probably occurred during the first few minutes following the burst. Referring to the permanent x-ray effects data for the low-loss type B shown in Figure 9, paragraph 3.2.2, after a dose of 20 kilorads and an induced change in transmission of 58 dB/km, the transmission improved by only about 8 dB/km 15 min after the irradiation was stopped. The annealing rate of transmission losses induced by the neutron irradiation is therefore much greater than that of the x-ray induced losses.

3.3.3 PLASTIC FIBERS

Only the Dupont Crofon® was tested for its response to neutrons. The results of the irradiations are shown in Figure 25. The slope relative to gamma dose of the line from the origin to the data point at 5.45×10^{11} n/cm^2 and 120 rads is 0.14 dB/km-rad; for the line to the point at 1.66×10^{12} n/cm^2 the slope is 0.18 dB/km-rad. These slopes are roughly three times the initial induced loss

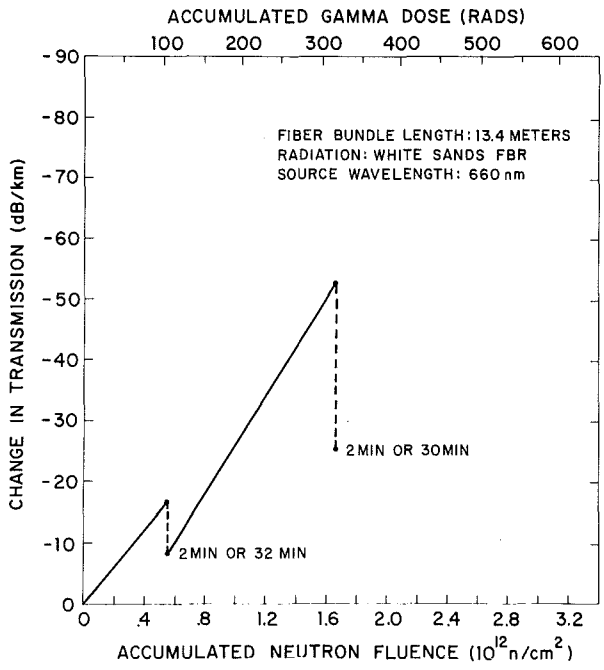

Figure 25. Change in Transmission Versus Neutron Fluence, Dupont Crofon® 1110

(0.055 dB/km-rad) found for this fiber in the permanent x-ray effects tests. The observed changes in transmission were therefore caused by both the neutrons and the gamma radiation, with the neutrons producing most (60 to 70 percent) of the changes.

It was found in the permanent x-ray tests of this fiber that the annealing rate of the induced loss is a function of the loss. Since the changes in transmission produced during the neutron irradiations were less than those for which annealing was observed in the permanent x-ray tests, a direct comparison of annealing rates between the two tests is not possible. Annealing of the losses induced in the Crofon® by the reactor radiation is unusual in that it apparently reached its limit within 2 min following a reactor burst. This is indicated in Figure 25 which shows that the change in transmission measured 2 min after a reactor burst was the same as that measured 30 min later. It cannot necessarily be concluded from this, however, that the annealing rate following neutron irradiation is greater than that following irradiation with x-rays.

3.3.4 CERIUM DOPED FIBERS

Three cerium doped glass fibers, identical to those used for the permanent x-ray effects tests, were tested. Some anomalous results, indicative of erratic optical coupling between the fiber and either the LED light source or photodetector, were found when the 0.2 percent cerium doped fiber data was analyzed. Therefore,

fore, only the results obtained for the 0.1 and 0.3 percent doped fibers are presented here. These are shown in Figures 26 and 27 respectively.

For the 0.1 percent cerium doped fiber, the average slope, relative to gamma dose, of the lines drawn between the data points in Figure 26 is 0.59 dB/km-rad. This is three times the initial rate of induced loss (0.2 dB/km-rad) found in the permanent x-ray effects tests of this fiber. Similarly, for the 0.3 percent doped fiber the average slope of the lines in Figure 27 is 0.23 which is also about three times the initial rate of induced loss (0.079 dB/km-rad) found in the x-ray tests. It can therefore be concluded that, like the plastic fiber, the changes in transmission observed in these fibers were due to both the neutrons and gamma radiations, with 60 to 70 percent of the changes being caused by the neutrons.

Although the data show that the 0.3 percent cerium doped fiber is significantly less sensitive to losses induced by neutrons than the 0.1 percent doped fiber, no specific conclusions can be drawn from the data regarding the relative rates of annealing of the induced losses. Also, the changes in transmission produced in the fibers by the reactor radiations were less than those for which annealing was observed in the permanent x-ray tests, so it is not possible to make a valid comparison between annealing results for the neutron and x-ray tests.

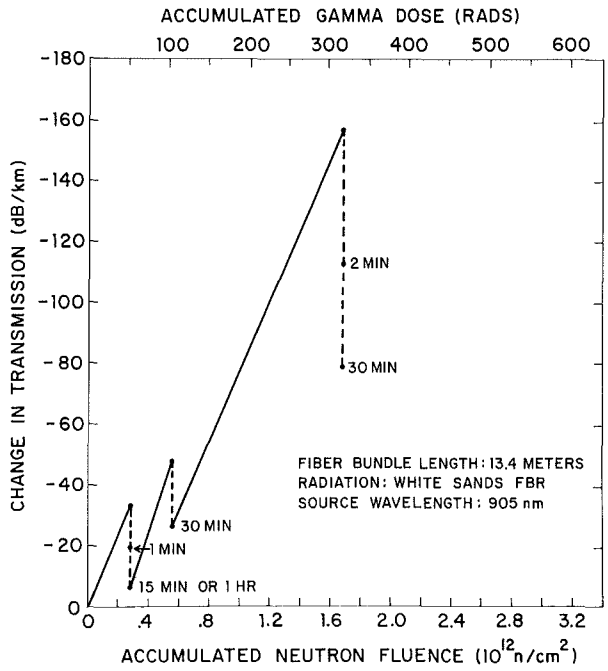

Figure 26. Change in Transmission Versus Neutron Fluence, 0.1 percent Cerium Doped Glass Fiber

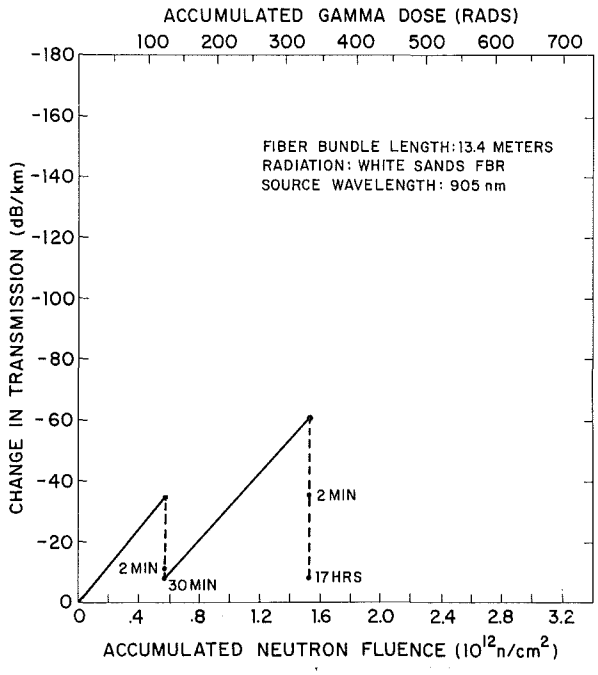

Figure 27. Change in Transmission Versus Neutron Fluence, 0.3 percent Cerium Doped Glass Fiber

3.3.5 RELATIVE SENSITIVITIES OF FIBERS TO NEUTRONS

If we assume that the initial rates of induced loss found for x-rays can be applied linearly to the gamma radiation that accompanied the neutrons during the reactor irradiations of the fibers, the relative sensitivities of the fibers to neutron induced losses can be estimated. Using this assumption the change in transmission caused by the gamma radiation alone is given by:

$$\Delta T_\gamma = rD \tag{4}$$

where

ΔT_γ = the change in transmission caused by gamma radiation

r = initial rate of induced loss for x-rays as given in Table I paragraph 3.2.5

D = the dose due to gamma radiation during a reactor burst.

The change in transmission caused by the neutrons alone is then:

$$\Delta T_n = \Delta T_{n\gamma} - rD \tag{5}$$

where

ΔT_n = the change in transmission caused by neutrons

$\Delta T_{n\gamma}$ = the change in transmission produced by the mixed neutron-gamma radiation.

Dividing ΔT_n by Φ, the neutron fluence in units of 10^{12} n/cm^2 for a given reactor burst, gives the change in transmission produced in a fiber per unit neutron fluence. These calculations were performed for the first reactor burst to which each fiber was exposed and the results are shown in Table 2. In Table 2 $\Delta T/\Phi$ is in units of dB/km per 10^{12} neutrons/cm^2. Results for the Corning 5011 fiber are not given in the table because no initial rate of induced loss for x-rays had been measured for it.

Table 2. Comparison of Sensitivities of Fibers to Neutrons

Fiber Type	Fiber Designation	Neutron Sensitivity $\Delta T/\Phi$
Commercial Glass	Bendix K2K	161
Low-Loss Fused Silica	Corning Low-Loss "B"	254
	Corning I-279	~ 0
Plastic	Dupont Crofon®	19.9
Cerium Doped	0.1 percent Ce	79.2
	0.3 percent Ce	44.7

With the exception of the Corning low-loss type B, the different types of fiber are in the same order of sensitivity to neutron induced losses as for x-ray induced losses. The high value of $\Delta T/\Phi$ obtained for the low-loss type B fiber is difficult to accept, particularly in view of the fact that a similar fiber like the Corning I-279 showed no detectable change in transmission when exposed to a greater neutron fluence (paragraph 3.3.2). Since there is nothing in the data to justify rejecting this high value of $\Delta T/\Phi$, one can only speculate regarding the reasons for it. Table 2 is presented solely for the purpose of comparing the measured neutron responses of the fibers tested, and no additional implications should be applied to the listed values of $\Delta T/\Phi$. Specifically this method used to calculate $\Delta T/\Phi$ is not intended to imply that the complex effects, produced by the simultaneous irradiation of the fibers by neutrons and gamma rays, can be easily separated.

3.4 Transient X-Ray Effects

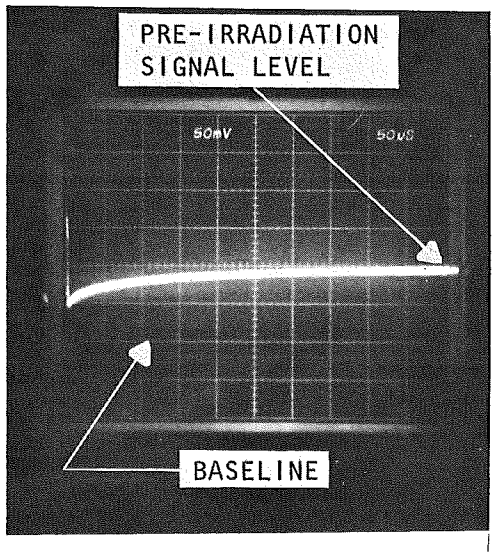

Figure 28. Signal Transmitted by 4.5 m Length of Dupont Crofon® Plastic Fiber Irradiated With 1200 rad, 20 nsec X-ray Pulse

The different types of fibers tested all had a common form of response when subjected to intense x-ray pulses. The form of this response is illustrated in Figure 28 which is a photograph of the oscilloscope trace of the signal transmitted by a 4.5 m length (7.5 m including leads) of Dupont Crofon® plastic fiber when it was irradiated by a 1200 rad, 20 nsec x-ray pulse. For this irradiation the oscilloscope trace position was set two major divisions (centimeters) below the graticle centerline with no input signal. The signal amplitude from the photo-detector prior to irradiation was 105 mv, putting the oscilloscope trace 1 mm above the centerline. The photograph shows a pulse, greater in amplitude than the pre-irradiation signal, at the beginning of the trace. This pulse is due to fluorescent radiation produced in the fiber by the x-rays. Following the fluorescence pulse the signal amplitude has dropped to about 50 percent of its original value, showing a radiation induced change in the transmission of the fiber. The signal level, and therefore the transmission, then approaches its pre-irradiation value over a period of 500 μsec.

Because all of the fibers tested showed both a radiation induced transient change in transmission and a fluorescent pulse, the results of the transient x-ray tests are classified according to these two characteristics instead of according to fiber types as was done in previous sections.

3.4.1 TRANSIENT CHANGE IN TRANSMISSION

The initial magnitude, rate of recovery, and degree of recovery of the transient change in transmission differed considerably among the types of fibers tested. To characterize these differences, the amplitude of the signal transmitted as a function of time following an x-ray pulse was determined for each fiber from oscilloscope photographs similar to that shown in Figure 28. Using the signal amplitude measured before irradiation and applying Eq. (1), paragraph 3.1, a table of values of the induced change in transmission in dB/km versus time was

obtained for each fiber. These results were then normalized to the dose received by the fibers during irradiation. It was found possible to fit these data to within 10 percent with a relation of the form*

$$\Delta T = Ae^{-t/\tau_1} + Be^{-t/\tau_2} + C \qquad (6)$$

where

ΔT = induced change in transmission per unit dose (dB/km-rad)

t = time after x-ray pulse (milliseconds).

A, B, C, τ_1 and τ_2 are constants characteristic of the fiber.

The characteristic constants found for the fibers tested are shown in Table 3.

Table 3. Characteristic Constants of Eq. (6) for Transient Radiation Induced Change in Transmission of Fibers

Fiber Type	Fiber Designation	Dose	A	B	C	τ_1	τ_2
Commercial Glass	Bendix K2K	93	7.17	6.77	3.95	18.9	0.203
	Corning 5011 (note)	92	11.1	-	5.51	2.49	-
Low-loss Fused Silica	Corning Low-loss "A"	230	1.03	1.04	0.605	27.0	0.397
	Corning I-279	1000	0.161	0.213	0	0.658	0.041
Plastic	Dupont Crofon®	1200	0.259	0.347	0	0.338	0.382
	I.F.O. 1032	940	0.167	0	0	0.0223	0
Cerium Doped	0.1 Percent Ce	120	0.633	0.460	0.156	16.1	0.306
	0.2 Percent Ce	160	0.441	0.276	0.0648	11.3	0.266
	0.3 Percent Ce	150	0.339	0.389	0.032	15.4	0.306

Units: Dose in Rads (Si)

A, B, C in dB/km-rad

τ_1, τ_2 in milliseconds

Note: Insufficient data for complete fit. Applies only for $\tau \leq 0.5$ msec.

*Attempts were made to fit the transient data with functions having the form At^{-a} which was found to apply to the long term recovery of induced losses for the plastic fibers (paragraph 3.2.3), but it was found that this type of function could be applied only to fairly limited ranges of time.

The values of the constants shown in Table 3 were obtained from least squares fits to data covering periods up to 10-30 msec after the x-ray pulses. For most of the fibers tested the induced changes in transmission continued to anneal out over much longer time periods. This long-term annealing, similar to that observed in the permanent x-ray effects tests, was not considered appropriate for inclusion in the transient radiation effects test results. Equation (6), along with the given constants, is therefore not necessarily representative of the transient responses of the fibers for times greater than the order of 10 msec after irradiation with an x-ray pulse.

The doses listed in Table 3 are those received by the fibers from a single x-ray pulse during the tests. These are the doses used to normalize the measured changes in transmission before fitting the data to Eq. (6). The normalization was performed in order to make a comparison of the transient responses of the different fibers possible even though they had not received the same doses. (Higher doses were required for some of the fibers in order to obtain changes in signal amplitude sufficient for accurate measurements to be made). This procedure implies that the induced changes in transmission are proportional to dose. Although tests were performed with the Corning low-loss type A fiber at doses of 30, 230, and 700 rads that showed this proportionality, it does not necessarily hold for all fibers or over all dose ranges. However, the assumption of proportionality between dose and induced change in transmission can be eliminated from the information given in the table by multiplying the constants A, B, and C by the appropriate dose. Applying Eq. (6) will then give the changes in transmission, in dB/km, actually observed during the tests.

The magnitude of the initially induced change in transmission and the rate at which the induced change recovers may be used as criteria for ranking the fibers according to their resistance to transient radiation effects. The sum of the constants A, B, and C gives a measure of the initially induced change in transmission. Based on this criterion alone, Table 3 shows the International Fiber Optics 1032 plastic fiber to be the most resistant to transient effects. This is followed by the Corning I-279 (germanium doped fused silica), the Dupont Crofon® (plastic), the cerium doped fibers, the Corning low-loss type A (titanium doped fused silica), and the commercial glass fibers. The smaller the constants τ_1 and τ_2, the faster the rate of recovery of the induced change in transmission. Based on the tabulated values of τ_1 and τ_2, ignoring the Corning 5011 results which were based on a limited amount of recovery time data, the fibers rank in the same order of radiation resistance except that the Dupont Crofon® shows a faster recovery time than the Corning I-279.

3.4.2 FLUORESCENT PULSE

Figure 29 shows an oscilloscope photograph of the signal produced by the fluorescent pulse generated in a Corning I-279 single fiber. For this photograph, a 9.8 m length (total length 11.4 m including leads) of the fiber was exposed to a 1000 rad, 20 nsec x-ray pulse. There was no light input to the fiber and the zero-signal position of the oscilloscope trace was set one major division (centimeter) below the graticle centerline. The fluorescence signal has its maximum amplitude at the beginning of the trace, corresponding to the incidence of the x-ray pulse. The amplitude decreases exponentially, as determined by a least-squares fit to data taken from the photograph, toward the zero signal level during a period of over 2 μsec.

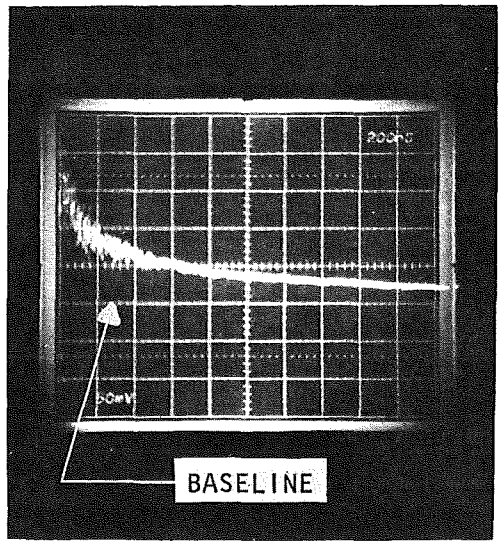

Figure 29. Signal Produced by Fluorescent Pulse Generated in 9.8 m Length of Corning I-279 Single Fiber Irradiated With 1000 rad, 20 nsec X-ray Pulse

The Corning I-279 single fiber is the only fiber tested for which it was possible to obtain complete temporal data on the x-ray generated fluorescent pulse. The fluorescence produced in the other fibers (which were tested as jacketed bundles containing many single fibers) was of sufficient magnitude to overload the photodetector even at the lowest dose (20 rads per pulse) available from the flash x-ray machine. However, it was possible to obtain some information on the fluorescence produced in the other fibers by measuring the dynamic overload characteristics of the photodetector and comparing these with the signals produced by the fluorescence during the irradiations. The overload characteristics of the photodetector were measured by using a laser diode that produced a 100 nsec wide pulse in combination with neutral density filters to generate a wide range of signals from the photodetector. It was found that as the intensity of the light input to the photodetector was increased, the output signal amplitude increased linearly up to a maximum beyond which only the width of the output signal increased. A direct correlation was found between the width of the photodetector output signal and the intensity of the light input and this was used to determine the amplitudes of the fluorescent pulses obtained from the fibers. The changes in the photodetector output signal decay time under overload conditions were also measured and the results used to correct the observed decay times of the fluorescent pulses.

The effective radiant intensity of the fluorescence emitted at the ends of the fibers was estimated from the properties of the photodetector (Texas Instruments TIXL79). The detector had a responsivity of 2×10^5 volts/watt at 900 nm and a sensitive area of 4.6×10^{-3} cm^2. The distance from the detector window, against which the fibers were butted, to the sensitive area was 0.19 cm giving a solid angle of 0.127 sr. The effective intensity at 900 nm was therefore obtained from:

$$I = \frac{V}{2 \times 10^5 \times 0.127} = 3.94 \times 10^{-5} V \tag{7}$$

where

I = intensity in microwatts/steradian

and

V = photodetector signal amplitude in microvolts

In order to compare the intensities of the fluorescence generated in the different fibers, the following normalization procedure was performed. Let i be the fluorescent intensity generated per unit length and trapped in the fiber. Assuming exponential absorption of the fluorescence radiation, the observed intensity at the end of the fiber is:

$$I = \int_0^L i e^{-\alpha x} dx = \frac{i}{\alpha}(1 - e^{-\alpha L}) \tag{8}$$

where

I = intensity at end of fiber

i = intensity generated and trapped per unit length of fiber

α = absorption coefficient

L = length of fiber

x = distance from end of fiber at which fluorescence is generated.

From (8) we obtain

$$i = \frac{I\alpha}{1 - e^{-\alpha L}} \tag{9}$$

which normalizes the observed fluorescent intensity to fiber length. The value of "α" is directly related to the attenuation of the fiber expressed in dB/km. If "L" is expressed in meters

$$\alpha = 2.3 \times 10^{-4} A \tag{10}$$

where

A = fiber attenuation in dB/km

α = absorption coefficient in m^{-1}

In evaluating "α", the approximate intrinsic attenuations of the fibers were used. This presumes that no radiation induced losses in the transmissions of the fibers coincided with the generation of the fluorescent pulses.

It was found that the intensity of the fluorescence generated in the plastic fibers was a linear function of the dose rate to which they were exposed. Assuming this was also true for the glass fibers, the values of "i" obtained from Eq. (9) were divided by the dose rates to which the fibers were exposed. An additional division by the numbers of fibers in the irradiated bundles completed the normalization process, giving:

$$i_n = \frac{I\alpha}{(1 - e^{-\alpha L})\dot{D} \cdot N} \tag{11}$$

where

i_n = fluorescent intensity per unit length and dose rate per fiber

$\dot{D}$ = dose rate

N = number of fibers in bundle

Table 4 lists i_n for the fibers tested along with the values of the parameters used in the calculations. Also listed in Table 4 are the decay times constants "τ" for the fluorescent pulses. Here it is assumed that the fluorescence decays as:

$$I = I_0 e^{-t/\tau} \tag{12}$$

where

I_0 = initial intensity of fluorescence

t = time after x-ray pulse.

The number of fibers per bundle (N) listed in Table 4 were estimated from the manufacturers' specifications of fiber and bundle diameters. Where N is shown as 100 or more the numbers were rounded off to the nearest 100. All of the fibers in a bundle were not necessarily continuous throughout the length of

Table 4. Fluorescent Pulse Characteristics

Fiber Type	Fiber Designation	i_n	τ	I	$\dot{D}$	L	N	A
Commercial Glass	Bendix K2K	5.3×10^{-2}	3.1	2.8×10^{5}	4.65×10^{3}	4.7	400	1000
	Corning 5011	4.6×10^{-3}	2.6	5.1×10^{4}	4.6×10^{3}	5.2	800	1000
Fused Silica	Corning low-loss "A"	3.6×10^{-4}	0.4	2.1×10^{2}	1.35×10^{3}	4.6	100	100
	Corning I-279	6.9×10^{-6}	0.38	3.3	5×10^{4}	9.8	1	10
Plastic	Dupont Crofon®	9.7×10^{-4}	~0	1.3×10^{2}	3.3×10^{3}	4.5	16	1200
	I.F.O. 1032	1.2×10^{-3}	0.3	1.4×10^{2}	1.65×10^{3}	4.5	32	1500
Cerium Doped Glass	0.1 Percent Ce	1.5×10^{-3}	6.8	3.3×10^{3}	6.15×10^{3}	13.4	100	1200
	0.2 Percent Ce	2.2×10^{-3}	7.8	6.2×10^{3}	8.05×10^{3}	13.1	100	1200
	0.3 Percent Ce	1.5×10^{-3}	6.1	3.3×10^{3}	7.65×10^{3}	13.4	100	1500

Units - -

i_n : μW/steradian-megarad/sec-m-fiber
τ : μsec
I : μW/steradian
$\dot{D}$: megarads/sec
L : m
A : dB/km

the bundle. A particularly extreme example of this is the Corning low-loss type A, which is a fairly brittle fiber and easily broken. It had only about 20 percent of the fibers conducting light through the length of the bundle. Since fluorescence is generated throughout the fibers regardless of whether or not they are broken, the effects of incomplete continuity of a bundle could not be reasonably accounted for. All of the fibers in a bundle were therefore assumed to be conducting when i_n was computed. The lengths of fiber (L) shown in the table are the lengths actually exposed to the x-ray pulses. The total fiber lengths used in the tests were about 3 m longer, the additional fiber being used as leads between

the irradiated coil and the photodetector and source. These leads were assumed lossless when calculating i_n.

Except in the case of the Corning I-279 fiber, the values of I (and therefore i_n) and τ shown in Table 4 are only approximate. This is because of the corrections required in the data to account for the overloading of the photodetector. Assuming the values of i_n are valid within a factor of two, all of the fibers apparently emit roughly the same amount of fluorescent radiation per unit length and incident dose rate with the exceptions of the Bendix K2K and the fused silica fibers. No explanation can be given for the much larger fluorescence observed from the Bendix fiber than from the others. The lower normalized fluorescent intensity emitted from the fused silica fibers, however, could be explained by the fact that the optical acceptance angle for this type of fiber is four to five times smaller than the acceptance angles of the other fibers. Fluorescence radiation generated in the fused silica fibers is therefore more likely to escape through the fiber surfaces rather than being conducted along the fiber. The much greater fluorescent intensity observed from the Corning low-loss type A fiber bundle than from the Corning I-279 single fiber could be the result of fluorescence radiation escaping through the surfaces of the fibers and being pickup-up at the proper acceptance angle by other fibers in the bundle. This greater "collection efficiency" of the fiber bundle compared to the single fiber would result in an apparently higher level of fluorescence per fiber.

The decay time constants of the fluorescent pulses for the fused silica and plastic fibers are an order of magnitude shorter than for the commercial and cerium doped glass fibers. Therefore, even if all the different types of fiber emitted the same intensity of fluorescence, the fused silica and plastic fibers would be preferable for use in a transient radiation environment because of the much shorter duration of the fluorescent pulses that might be produced in them.

3.5 Summary of Results

To review the significance of the test results, they will be applied to estimate the effects of radiation on 30 m lengths of the fibers tested. Table 5 shows the doses required to reduce the transmissions of the fibers to 50 percent of their pre-irradiation values; that is, an induced change in transmission of -100 dB/km for a 30 m length. The results shown in Table 5 do not take into account annealing of the induced losses and are taken directly from plots of the permanent x-ray effects test data.

These results clearly show the superior resistance of the germanium doped fused silica fiber (Corning low-loss type B) to x-radiation induced losses in transmission.

Table 5. X-Ray Dose Required to Reduce the Transmission of a 30 m Length of Optical Fiber to 50 Percent of its Original Value

Fiber	Dose (Rads)
Bendix K2K	38
Rank Hi-Tran	38
Schott LK	65
Corning Low-Loss "A"	105
0.1 Percent Ce Doped	500
0.2 Percent Ce Doped	1100
0.3 Percent Ce Doped	1500
Dupont Crofon®	5000
I.F.O. 1032	8000
Corning Low-Loss "B"	40,000

Table 6 shows the estimated neutron fluences required to reduce the transmissions of 30 m lengths of fiber to 50 percent of the pre-irradiation values. The results shown in this table were derived from the neutron sensitivities ($\Delta T/\Phi$) shown in Table 2, paragraph 3.2.5, and are irrespective of annealing effects.

Table 6. Neutron Fluence Required to Reduce the Transmission of a 30 m Length of Optical Fiber to 50 percent of its Original Value

Fiber	Neutron Fluence (10^{12} neutrons/cm^2)
Corning	0.39
Bendix K2K	0.62
0.1 Percent Ce Doped	1.3
0.3 Percent Ce Doped	2.2
Corning I-279	> 3
Dupont Crofon	5

As discussed in paragraph 3.2.2, there is a conflict in the neutron test results obtained for the two germanium doped fused silica fibers. The Corning low-loss type B fiber was found to be the most sensitive to neutron damage, as Table 6 shows, while the Corning I-279 fiber showed no detectable change in transmission after exposure to 3×10^{12} neutrons/cm^2. Because this difference in neutron sensitivities could not be explained except on the basis of a possible lower sensitivity for the Corning I-279 tests, the Dupont Crofon® plastic fiber is shown in the table as the least sensitive to neutron induced transmission losses.

Table 7 shows the times required for the transmissions of 30 m lengths of fiber to recover to 50 percent of their original values after exposure to a 1000 rad pulse of x-rays.

The recovery times were computed from Eq. (6) and the constants listed in Table 3, of paragraph 3.3.1. Those fibers for which the recovery times would exceed one min are not included in Table 7.

Table 7. Time Required for the Transmission of a 30 m Length of Fiber to Recover to 50 percent of its Original Value Following a 1000 Rad X-Ray Pulse

Fiber	Recovery Time (milliseconds)
0.2 Percent Ce Doped	29
0.3 Percent Ce Doped	25
Dupont Crofon®	0.32
Corning I-279	0.31
I.F.O. 1032	0.011

The International Fiber Optics 1032 plastic fiber has a recovery time that is shorter by more than an order of magnitude than its closest competitors, the Dupont Crofon® plastic fiber and the Corning I-279 germanium doped fused silica fiber. The 0.1 percent cerium doped glass fiber was excluded from the Table 7 because of its long recovery time. This, along with the results presented for the other cerium doped fibers, shows that cerium doping can improve the transient radiation effects properties of glass fibers as well as their resistance to permanent radiation induced transmission losses.

Equation (11) in paragraph 3.3.2, was solved for the fluorescent radiant intensity per unit dose rate per fiber ($I/N \cdot \dot{D}$) that would be emitted at the ends of 30 m lengths of the fibers when exposed to x-ray pulses. The data shown in Table 4, paragraph 3.3.2, were used to evaluate $I/N \cdot \dot{D}$ and the results are

Table 8. Fluorescent Radiant Intensity at the End of a 30 m Length of Fiber Exposed to an X-Ray Pulse

Fiber	$I/N \cdot \dot{D}$	τ (μsec)
Bendix K2K	0.23	3.1
Corning 5011	0.02	2.6
0.2 Percent Ce Doped	8×10^{-3}	7.8
Corning Low-Loss "A"	7.8×10^{-3}	0.4
0.1 Percent Ce Doped	5.4×10^{-3}	6.8
0.3 Percent Ce Doped	4.3×10^{-3}	6.1
I.F.O. 1032	3.5×10^{-3}	0.3
Dupont Crofon®	3.5×10^{-3}	~ 0
Corning I-279	2×10^{-4}	0.38

Units of $I/N \cdot \dot{D}$: μW/steradian-megarad/sec-fiber

listed in Table 8. The fluorescent pulse decay times (τ) listed in Table 4 are also shown here for comparison purposes. Comparison of the values of $I/N \cdot \dot{D}$ in Table 8 with the values of i_n—the fluorescent intensity per fiber per unit length and dose-rate—in Table 4 shows that the length of fiber considered has a significant effect on the relative intensity of the fluorescent radiation emitted from the end of the fiber. For example, the ratio of the value of i_n for the Dupont Crofon® to that for the Corning I-279 is 141, while the ratio of the values of $I/N \cdot \dot{D}$ for the 30 m lengths is 17.5. This is because the greater attenuation of the Crofon® reduces the amount of fluorescent radiation reaching the end of the fiber, compensating for the higher intensity of fluorescence generated and trapped per unit length. The lower intrinsic fluorescent emission of the fused silica fibers is therefore negated to some degree in long lengths of fiber because of their lower intrinsic attenuations.

The fused silica and plastics fibers have the shortest fluorescent pulse decay time constants. Table 8 shows that the decay time constants are dependent only on the type of fiber and do not correlate with the intensity of fluorescence.

In summarizing test results, germanium doped fused silica fibers appear to be the most radiation resistant of the fibers tested. The next most resistant to radiation damage are the plastic fibers, which have some advantages in faster recovery of transient induced transmission losses and lower neutron induced losses. The cerium doped glass fibers are more than an order of magnitude more resistant to radiation induced losses than the commercial glass fibers. The latter are very radiation sensitive and essentially unusable in radiation environments.

4. CONCLUSIONS AND RECOMMENDATIONS

The germanium doped fuse silica fibers, which were found to be the most resistant to radiation induced transmission losses, were developed primarily for their very low intrinsic attenuations so that they could be used as transmission lines in lengths of the order of kilometers. These fibers appear at present to be the most suitable for use where long lengths are required such as in ground based communication and data transmission systems. They have some disadvantages, however. Their cost per unit length is about ten times that of other glass fibers; they are less flexible than other types of fiber, which causes a higher breakage rate; and their numerical aperture is lower, making efficient coupling to light sources and detectors more difficult. These factors, particularly the higher cost, make consideration of other types of fiber worthwhile in applications, such as in aircraft control and communication systems, where continuous lengths of only a few tens of meters are required.

The plastic fibers, which showed a higher initial rate of radiation induced transmission losses than the germanium-doped fused silica fibers, were found to be superior to the others in their rate of recovery from transient x-ray induced losses and their resistance to neutron induced losses. Their cost per unit length is only about 10 percent of that of the lowest priced glass fibers. These factors may make them useful in systems in which their less desirable properties can be tolerated. One of these properties is their extremely high attenuation in the infrared, which makes them practically useless in this region of the spectrum where operation is desirable because of the availability of more efficient solid state light sources and detectors and because of greater security. The plastic fibers have poor thermal properties, their upper temperature tolerance limit being only about $80^{\circ}C$. They have low resistance to chemicals and moisture, and their intrinsic losses at their optimum operating wavelengths are high (1200-1500 dB/km).

The cerium doped glass fibers show some potential for application in manned systems. The 0.3 percent cerium doped fiber tested showed an induced change in transmission of -125 dB/km (a decrease to 42 percent of the original transmission for a 30 m length) after receiving an x-ray dose of 2000 rads, the assumed tolerance level for manned systems. These fibers have all of the cost advantages and favorable physical properties of standard commercial glass fibers, but they have relatively high intrinsic attenuations of over 1200 dB/km.

The significance of the fluorescent pulses generated in the fibers during the transient x-ray effects tests should be considered in view of the fact that, as mentioned in paragraph 2.2 "Experimental Setup", the photodetector was shielded by 10 cm of lead during the tests. This was necessary because even though the detector was located in an area where it received doses from the x-ray pulses

more than two orders of magnitude lower than the fibers that were being tested, without the shielding the radiation produced intense signals from the photodetector similar to those observed during optical overloading. Since it is unlikely that phtodetectors used in systems employing fiber optics would be so heavily shielded, the magnitudes of false signals caused by radiation induced fluorescence in the fibers may be of little consequence compared to the false signals produced in the detectors.

Considering the above, the following recommendations are made:

(1) Continue development of the germanium doped fused silica fibers to lower their cost and improve their mechanical properties.

(2) Develop cerium doped glass fibers with intrinsic attenuations below 1000 dB/km.

(3) Investigate new materials that could be used to produce plastic fibers with improved optical and thermal properties.

(4) Develop photodetectors which maximize the ratio of optical sensitivity to x-ray sensitivity.

These conclusions and recommendations are based only on the limited tests reported here. There are many other aspects of the problem of the effects of radiation on fiber optics, and optical materials in general, that must continue to be investigated in order to improve our understanding of the interaction of nuclear and space radiation with fiber optic systems.